# An energy-based analysis of reduced-order models of (networked) synchronous machines

Stegink, T. W.; De Persis, C.; Van der Schaft, A. J.

*Published in:*
Mathematical and computer modelling of dynamical systems

*DOI:*
10.1080/13873954.2019.1566265



*Publication date:*
2019

Taylor & Francis
Taylor & Francis Group

Mathematical and Computer Modelling of Dynamical Systems

Methods, Tools and Applications in Engineering and Related Sciences

ISSN: 1387-3954 (Print) 1744-5051 (Online) Journal homepage: https://www.tandfonline.com/loi/nmcm20

# An energy-based analysis of reduced-order models of (networked) synchronous machines

T. W. Stegink, C. De Persis & A. J. Van Der Schaft

**To cite this article:** T. W. Stegink, C. De Persis & A. J. Van Der Schaft (2019) An energy-based analysis of reduced-order models of (networked) synchronous machines, Mathematical and Computer Modelling of Dynamical Systems, 25:1, 1-39, DOI: 10.1080/13873954.2019.1566265

**To link to this article:** https://doi.org/10.1080/13873954.2019.1566265



Published online: 12 Feb 2019.

MATHEMATICAL AND COMPUTER MODELLING OF DYNAMICAL SYSTEMS
2019, VOL. 25, NO. 1, 1–39
https://doi.org/10.1080/13873954.2019.1566265

Taylor & Francis
Taylor & Francis Group

ARTICLE



# An energy-based analysis of reduced-order models of (networked) synchronous machines

T. W. Stegink[a], C. De Persis[a] and A. J. Van Der Schaft[b]

[a]Engineering and Technology institute Groningen, University of Groningen, Groningen, The Netherlands; [b]Johann Bernoulli Institute for Mathematics and Computer Science, University of Groningen, Groningen, The Netherlands

**ABSTRACT**

Stability of power networks is an increasingly important topic because of the high penetration of renewable distributed generation units. This requires the development of advanced techniques for the analysis and controller design of power networks. Although there are widely accepted reduced-order models to describe the power network dynamics, they are commonly presented without details about the reduction procedure. The present article aims to provide a modular model derivation of multi-machine power networks. Starting from first-principle fundamental physics, we present detailed dynamical models of synchronous machines and clearly state the underlying assumptions which lead to some of the standard reduced-order multi-machine models. In addition, the energy functions for these models are derived, which allows to represent the multi-machine systems as port-Hamiltonian systems. Moreover, the systems are proven to be shifted passive, which permits for a power-preserving interconnection with other passive components.

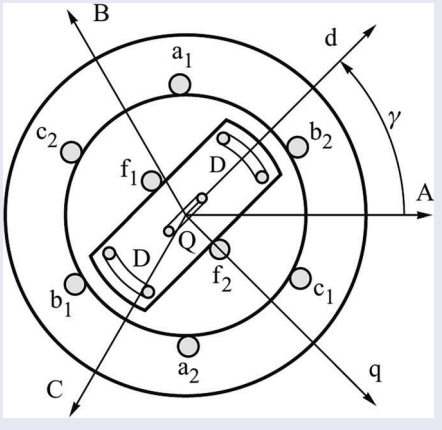


**ARTICLE HISTORY**
Received 5 April 2018
Accepted 10 December 2018

**KEYWORDS**
Power networks; synchronous machines; energy functions

**CONTACT** T. W. Stegink t.w.stegink@rug.nl Engineering and Technology institute Groningen, University of Groningen, Nijenborgh 4, Groningen, AG 9747, The Netherlands

# 1. Introduction

## 1.1. Problem statement/motivation

The control and stability of power networks has become increasingly challenging over the last decades. As renewable energy sources penetrate the grid, the conventional power plants have more difficulty in keeping the frequency around the nominal value, e.g. 50 Hz, leading to an increased chance of network failures or, in the worst case, even blackouts.

The current developments require a sophisticated stability analysis of more advanced models for the power network as the grid is operating more frequently near its capacity constraints. For example, using high-order models of synchronous machines that better approximate the actual system allows us to establish results on the stability of power networks that are more reliable and accurate.

However, in much of the recent literature, a rigorous stability analysis has been carried out only for low-order models of the power network which have a limited accuracy. For models of intermediate complexity, the stability analysis has merely been done for the linearized system. Hence, a novel approach is required to make a profound stability analysis of these more complicated models possible.

In this article, we propose a unifying energy-based approach for the modelling and analysis of multi-machine power networks which is based on the theory of port-Hamiltonian systems. Since energy is the main quantity of interest, the port-Hamiltonian framework is a natural approach to deal with the problem [1]. Moreover, it lends itself to deal with large-scale nonlinear multi-physics systems like power networks [2–5].

## 1.2. Literature review

The emphasis in the present article lies on the modelling and analysis of (networked) synchronous machines since they have a crucial role in the stability of power networks as they are the most flexible and have to compensate for the increased fluctuation of both the supply and demand of power. An advanced model of the synchronous machine is the first-principle model which is derived in many power-engineering books [6–8], see in particular [7], Chapter 11] for a detailed derivation of the model.

Modelling the first-principle synchronous (multi-)machine model using the theory of port-Hamiltonian systems has been done previously in [2]. However, in this work, stabilization of the synchronous machine to the synchronous frequency could not be proven. In [9] a similar model for the synchronous machine is used, but with the damper windings neglected. Under some additional assumptions, asymptotic stability of a single machine is proven using a shifted energy function. For multi-machine systems, however, stability could not be proven using a similar approach.

Summarizing, the complexity of the full-order model of the synchronous machine makes a rigorous stability analysis troublesome, especially when considering multi-machine networks, see also [10]. Moreover, it is often not necessary to consider the full-order model when studying a particular aspect of the electromechanical dynamics (e.g. operation around the synchronous frequency) [7].

On the other side of the spectrum, much of the literature using Lyapunov stability techniques rely on the second-order (non)linear swing equations as the model for the power network [7,11–17] or the third-order model as e.g. in [18]. For microgrids similar models are considered in which a Lyapunov stability analysis is carried out [19,20]. However, the models are often presented without stating the details on the model reduction procedure or the validity of the model. For example, the swing equations are inaccurate and only valid on a specific timescale up to the order of a few seconds so that asymptotic stability results have a limited value for the actual system [6–8,21].

Hence, it is appropriate to make simplifying assumptions for the full-order model and to focus on multi-machine models with intermediate complexity which provide a more accurate description of the network compared to the second- and third-order models [6–8]. In doing so, we explain how these intermediate-order models are obtained from the first-principle model and what the underlying assumptions are. Here we follow the lines of [7], where a detailed derivation of the reduced-order models is given.

### 1.3. Contributions

The main contribution of this chapter consists of establishing a unifying energy-based analysis of intermediate-order models of (networked) synchronous machines. In doing so, we first explain how these intermediate-order models are obtained from the first-principle model and highlight what the underlying assumptions are, and then how these synchronous machines are coupled through inductive lines. This part has a tutorial value where we follow the lines of [7], in which a detailed derivation of the reduced-order models is given. This forms the foundation of our second contribution which is the systematic procedure to obtain the energy functions of the reduced order multi-models. In particular, we show how the energy functions of the reduced order models are obtained from the first-principle model, which is represented in a very different set of variables and parameters, and that these energy functions contain a common factor which is often ignored in power system stability studies. Another key contribution is that, building on the expression of the energy functions (or Hamiltonians), port-Hamiltonian representations of various synchronous machine models are obtained which include the full-order model as well as the sixth-, third-, and classical second-order models. In particular, this reveals the sparse but nontrivial interconnection and damping structures of these systems, having the complexity mainly appearing in the expression of the Hamiltonian. Specifically for a realistic sixth-order model, we show that the system is dissipative by explicitly proving that the dissipation matrix is positive definite which is far from trivial. Finally, by exploiting the specific structure of the port-Hamiltonian systems (state-independent interconnection and damping structure), shifted passivity of the reduced order multi-machine models is proven. To the authors' best knowledge, except for our previous work [22], such shifted passivity properties have not been established for (4,5,6-)order models. This allows to consider such intermediate-order multi-machine models, having a quite accurate description of the power network dynamics, while permitting a rigorous (Lyapunov-based) stability analysis of nontrivial equilibria. This is in contrast with the current literature which mainly relies on linearization techniques for the stability analysis of such complex systems.

### 1.4. Outline

The remainder of the article is structured as follows. First, we state the preliminaries in Section 2. Then, in Section 3 the full-order first-principle model is presented and its port-Hamiltonian form is given. The model reduction procedure is discussed in Section 4 in which models of intermediate order are obtained. In Section 5 these models are used to establish multi-machine models, including the classical second-order model. Then, in Section 6 energy functions of the reduced order models are derived, which in Section 7 are used to put the multi-machine models in port-Hamiltonian form. Finally, Section 8 discusses the conclusions and possible directions for future research.

## 2. Preliminaries

### 2.1. Notation

The set of real numbers and the set of complex numbers are, respectively, defined by $\mathbb{R}, \mathbb{C}$. Given a complex number $\alpha \in \mathbb{C}$, the real and imaginary parts are denoted by $\Re(\alpha), \Im(\alpha)$, respectively. The imaginary unit is denoted by $j = \sqrt{-1}$. Let $\{v_1, v_2, \ldots, v_n\}$ be a set of real numbers, then $\mathrm{diag}(v_1, v_2, \ldots, v_n)$ denotes the $n \times n$ diagonal matrix with the entries $v_1, v_2, \ldots, v_n$ on the diagonal and likewise $\mathrm{col}(v_1, v_2, \ldots, v_n)$ denotes the column vector with the entries $v_1, v_2, \ldots, v_n$. Let $f : \mathbb{R}^n \to \mathbb{R}$ be a twice differentiable function, then $\nabla f(x)$ denotes the gradient of $f$ evaluated at $x$ and $\nabla^2 f(x)$ denotes the Hessian of $f$ evaluated at $x$. Given a symmetric matrix $A \in \mathbb{R}^{n \times n}$, we write $A > 0$ $(A \geq 0)$ to indicate that $A$ is a positive (semi-)definite matrix.

#### 2.1.1. Power network

Consider a power grid consisting of $n$ buses. The network is represented by a connected and undirected graph $\mathcal{G} = (\mathcal{V}, \mathcal{E})$, where the set of nodes, $\mathcal{V} = \{1, \ldots, n\}$, is the set of buses representing the synchronous machines and the set of edges, $\mathcal{E} \subset \mathcal{V} \times \mathcal{V}$, is the set of transmission lines connecting the buses where each edge $(i, k) = (k, i) \in \mathcal{E}$ is an unordered pair of two vertices $i, k \in \mathcal{V}$. Given a node $i$, then the set of neighbouring nodes is denoted by $\mathcal{N}_i := \{k \,|\, (i, k) \in \mathcal{E}\}$.

**Nomenclature**

| | |
|---|---|
| $\alpha$ | Voltage angle with respect to $dq0$-reference frame of the rotor. |
| $\delta$ | Rotor angle with respect to the synchronous rotating reference frame. |
| $\Delta\omega$ | Rotor frequency with respect to the synchronous rotating reference frame. |
| $\gamma$ | Rotor angle of the synchronous machine. |
| $\mathcal{B}$ | Incidence matrix of the network. |
| $\Psi_0$ | 0-axis stator winding flux linkage. |
| $\Psi_D$ | $d$-axis damper winding flux linkage. |
| $\Psi_d$ | $d$-axis stator winding flux linkage. |
| $\Psi_f$ | Field winding flux linkage. |
| $\Psi_g$ | Additional $q$-axis damper winding flux linkage. |
| $\Psi_Q$ | $q$-axis damper winding flux linkage. |
| $\Psi_q$ | $q$-axis stator winding flux linkage. |

| | |
|---|---|
| $\theta$ | Voltage angle with respect to the synchronous rotating reference frame. |
| $\omega$ | Rotor frequency. |
| $\omega_s$ | Synchronous frequency (e.g. 50 Hz). |
| $B_{ii}$ | Self-susceptance at node $i$. |
| $B_{ij}$ | Line susceptance between nodes $i$ and $j$. |
| $D$ | Asynchronous damping constant. |
| $d$ | Mechanical damping constant. |
| $E'_d$ | $d$-axis component of the transient internal emf. |
| $E''_d$ | $d$-axis component of the subtransient internal emf. |
| $E'_q$ | $q$-axis component of the transient internal emf. |
| $E''_q$ | $q$-axis component of the subtransient internal emf. |
| $I_0$ | 0-axis stator winding current. |
| $I_D$ | $d$-axis damper winding current. |
| $I_d$ | $d$-axis stator winding current. |
| $I_f$ | Field winding current. |
| $I_g$ | Additional $q$-axis damper winding current. |
| $I_Q$ | $q$-axis damper winding current. |
| $I_q$ | $q$-axis stator winding current. |
| $p$ | Angular momentum. |
| $R_s$ | Stator winding resistance. |
| $T'_{doi}$ | $d$-axis open-circuit transient time constant. |
| $T''_{doi}$ | $d$-axis open-circuit subtransient time constant. |
| $T_{dq0}$ | The $dq0$-transformation or Park transformation. |
| $T'_{qoi}$ | $q$-axis open-circuit transient time constant. |
| $T''_{qoi}$ | $q$-axis open-circuit subtransient time constant. |
| $V_d$ | $d$-axis component of the external emf (of the synchronous machine). |
| $V_q$ | $q$-axis component of the external emf (of the synchronous machine). |
| $X_{di}$ | $d$-axis synchronous reactance. |
| $X_{qi}$ | $q$-axis synchronous reactance. |
| $X'_{di}$ | $d$-axis transient reactance. |
| $X'_{qi}$ | $q$-axis transient reactance. |
| $X''_{di}$ | $d$-axis subtransient reactance. |
| $X''_{qi}$ | $q$-axis subtransient reactance. |

## 2.2. The *dq*0-transformation

An important coordinate transformation used in the literature on power systems is the $dq0$-transformation [2,7] or *Park transformation* [23 ] which is defined by

$$T_{dq0}(\gamma) = \sqrt{\frac{3}{2}} \begin{bmatrix} \cos(\gamma) & \cos(\gamma - \frac{2\pi}{3}) & \cos(\gamma + \frac{2\pi}{3}) \\ \sin(\gamma) & \sin(\gamma - \frac{2\pi}{3}) & \sin(\gamma + \frac{2\pi}{3}) \\ \frac{1}{\sqrt{2}} & \frac{1}{\sqrt{2}} & \frac{1}{\sqrt{2}} \end{bmatrix}. \tag{2.1}$$

Observe that the mapping Equation (2.1) is orthogonal, i.e. $T^{-1}_{dq0}(\gamma) = T^T_{dq0}(\gamma)$. The $dq0$-transformation offers various advantages when analyzing power system dynamics and is

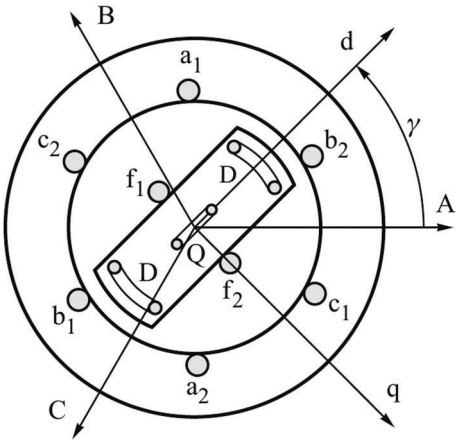


**Figure 1.** Schematic illustration of a (salient-pole) synchronous machine [7].

therefore widely used in applications. In particular, the $dq0$-transformation maps *symmetric* or *balanced* three-phase AC signals (see [24], Section 2] for the definition) to constant signals. This significantly simplifies the modelling and analysis of power systems, which is the main reason why the transformation Equation (2.1) is used in the present case. In addition, the transformation Equation (2.1) exploits the fact that, in a power system operated under symmetric conditions, a three-phase signal can be represented by two quantities [23].

For example, for a synchronous machine with AC voltage $V^{\mathrm{ABC}} = \mathrm{col}(V^A, V^B, V^C)$ in the static ABC-reference frame, see Figure 1, the $dq0$-transformation is used to map this AC voltage to the (local) $dq0$-coordinates as $V^{dq0} = \mathrm{col}(V_d, V_q, V_0) = T_{dq0}(\gamma)V^{\mathrm{ABC}}$. Note that the local $dq0$-reference is aligned with the rotor of the machine which has angle $\gamma$ with respect to the static ABC-reference frame, see again Figure 1. In case more that one synchronous machine is considered, then the voltage $V^{dq0^k}$ in local $dq0$-coordinates of machine $k$ can be expressed in the local $dq0$-coordinates of machine $i$ as

$$V^{dq0^i} = T_{dq0}(\gamma_i)V^{ABC^i} = T_{dq0}(\gamma_i)V^{ABC^k} = T_{dq0}(\gamma_i)T_{dq0}(\gamma_k)^T V^{dq0^k}. \tag{2.2}$$

An analogous expression can be obtained for relation between the currents $I^{dq0^i}$, and $I^{dq0^k}$. Here we can verify that

$$T_{dq0}(\gamma_i)T_{dq0}(\gamma_k)^T = \begin{bmatrix} \cos\gamma_{ik} & -\sin\gamma_{ik} & 0 \\ \sin\gamma_{ik} & \cos\gamma_{ik} & 0 \\ 0 & 0 & 1 \end{bmatrix}$$

where $\gamma_{ik} := \gamma_i - \gamma_k$ represents the rotor angle difference between synchronous machines $i$ and $k$ respectively.

### 2.3. Phasor notation

When considering operation around the synchronous frequency, the voltages and currents can be represented as phasors in the $dq$-coordinates rotating at the synchronous frequency. We use the following notation for the phasor[1] [7]:

$$\bar{V} = \sqrt{V_q^2 + V_d^2}\exp\left(j\arctan\left(\frac{V_d}{V_q}\right)\right) = \bar{V}_q + \bar{V}_d = V_q + jV_d,$$

$$\bar{I} = \sqrt{I_q^2 + I_d^2}\exp\left(j\arctan\left(\frac{I_d}{I_q}\right)\right) = \bar{I}_q + \bar{I}_d = I_q + jI_d,$$

which is commonly used in the power system literature [7,23]. Here the bar-notation is used to represent the complex phasor and we define $\bar{V}_q = V_q, \bar{V}_d = jV_d$ and a likewise $\bar{I}_q = I_q, \bar{I}_d = jI_d$ for the currents. In this case, the mapping between the voltages (and current) from one $dq$-reference frame to another is given by

$$\begin{aligned}\bar{V}^{dq^i} &= e^{-j\gamma_{ik}}\bar{V}^{dq^k} = (\cos\gamma_{ik} - j\sin\gamma_{ik})(V_q^{dq^k} + jV_d^{dq^k}) \\ &= V_q^{dq^k}\cos\gamma_{ik} + V_d^{dq^k}\sin\gamma_{ik} + j(V_d^{dq^k}\cos\gamma_{ik} - V_q^{dq^k}\sin\gamma_{ik}).\end{aligned} \tag{2.3}$$

By equating the real and imaginary parts, this exactly corresponds to the transformation Equation (2.2) as expected.

## 3. Full-order model of the synchronous machine

A synchronous machine is a multi-physics system characterized by both mechanical and electrical variables, i.e. an electromechanical system. Derived from physical first-principle laws, the dynamics can be described in terms of certain specific physical quantities such as the magnetic flux, voltages, angles, momenta and torques. The complete model can be described by a system of ordinary differential equations (ODE's) where the flux-current relations are represented by algebraic constraints. The generator rotor circuit is formed by a field circuit and three amortisseur circuits, which is divided into one $d$-axis circuit and two $q$-axis circuits. The stator is formed by three-phase windings which are spatially distributed in order to generate three-phase voltages at machine terminals. For convenience, magnetic saturation effects are neglected in the model of the synchronous machine. After applying the $dq0$-transformation $T_{dq0}(\gamma)$ on the ABC-variables with respect to the rotor angle $\gamma$, its dynamics in the $dq0$-reference frame is governed by the following ninth-order system of differential equations [2,7,8][2]:

$$\dot{\gamma} = \omega \tag{3.1a}$$

$$J\dot{\omega} = \Psi_q I_d - \Psi_d I_q - d\omega + \tau. \tag{3.1b}$$

$$\dot{\Psi}_d = -R_s I_d - \Psi_q\omega - V_d \tag{3.1c}$$

$$\dot{\Psi}_q = -R_s I_q + \Psi_d \omega - V_q \tag{3.1d}$$

$$\dot{\Psi}_0 = -R_s I_0 - V_0 \tag{3.1e}$$

$$\dot{\Psi}_f = -R_f I_f + V_f \tag{3.1f}$$

$$\dot{\Psi}_g = -R_g I_g \tag{3.1g}$$

$$\dot{\Psi}_D = -R_D I_D \tag{3.1h}$$

$$\dot{\Psi}_Q = -R_Q I_Q \tag{3.1i}$$

Here $V_d, V_q, V_0$ are instantaneous external voltages, $\tau$ is the external mechanical torque and $V_f$ is the excitation voltage. The rotor angle $\gamma$, governed by Equation (3.1a), is taken with respect to the static ABC-reference frame, see also Figure 1. The quantities $\Psi_d, \Psi_q, \Psi_0$ are stator winding flux linkages and $\Psi_f, \Psi_g, \Psi_D, \Psi_Q$ are the rotor flux linkages, respectively, and are related to the currents as [7]

$$\begin{bmatrix} \Psi_d \\ \Psi_f \\ \Psi_D \end{bmatrix} = \overbrace{\begin{bmatrix} L_d & \kappa M_f & \kappa M_D \\ \kappa M_f & L_f & L_{fD} \\ \kappa M_D & L_{fD} & L_D \end{bmatrix}}^{\mathcal{L}_d} \begin{bmatrix} I_d \\ I_f \\ I_D \end{bmatrix} \tag{3.2}$$

$$\begin{bmatrix} \Psi_q \\ \Psi_g \\ \Psi_Q \end{bmatrix} = \underbrace{\begin{bmatrix} L_q & \kappa M_g & \kappa M_Q \\ \kappa M_g & L_g & L_{gQ} \\ \kappa M_Q & L_{gQ} & L_Q \end{bmatrix}}_{\mathcal{L}_q} \begin{bmatrix} I_q \\ I_g \\ I_Q \end{bmatrix} \tag{3.3}$$

$$\Psi_0 = L_0 I_0, \tag{3.4}$$

where $\kappa = \sqrt{\frac{3}{2}}$, see also the nomenclature in Section 2.1. Note that in the $dq0$-coordinates, the inductor equations can be split up in each of the three axes, resulting into the three completely independent Equations (3.2)–(3.4). For a physically relevant model, the inductance matrices $\mathcal{L}_d, \mathcal{L}_q \in \mathbb{R}^{3\times 3}$ are assumed to be positive definite. An immediate observation from Equations (3.1e) and (3.4) is that the dynamics associated with the 0-axis is fully decoupled from the rest of the system. Therefore, without loss of generality, we omit this differential equation in the sequel and focus solely on the dynamics in the $d$- and $q$-axes.

**Remark 3.1** (Additional damper winding) Many generators, and in particular turbogenerators, have a solid-steel rotor body which acts as a screen in the $q$-axis [7]. It is convenient to represent this by the additional winding in the $q$-axis represented by the symbol $g$, see Equation (3.1g). However, for salient-pole synchronous generators, this winding is absent. For completeness, both cases are considered in this article.

### 3.1. Port-Hamiltonian representation

Inspired by the work [2], it can be shown that full-order model (3.1) admits a port-Hamiltonian representation, see [1] for a survey. More specifically, by defining the state vector $x = (\gamma, p, \Psi_d, \Psi_q, \Psi_f, \Psi_g, \Psi_D, \Psi_Q), p = J\omega$, the $dq$-dynamics of a single synchronous machine can be written in port-Hamiltonian form as

$$\begin{bmatrix} \dot{\gamma} \\ \dot{p} \\ \dot{\Psi}_d \\ \dot{\Psi}_q \\ \dot{\Psi}_f \\ \dot{\Psi}_g \\ \dot{\Psi}_D \\ \dot{\Psi}_Q \end{bmatrix} = \begin{bmatrix} 0 & 1 & 0 & 0 & 0 & 0 & 0 & 0 \\ -1 & -d & \Psi_q & -\Psi_d & 0 & 0 & 0 & 0 \\ 0 & -\Psi_q & -R_s & 0 & 0 & 0 & 0 & 0 \\ 0 & \Psi_d & 0 & -R_s & 0 & 0 & 0 & 0 \\ 0 & 0 & 0 & 0 & -R_f & 0 & 0 & 0 \\ 0 & 0 & 0 & 0 & 0 & -R_g & 0 & 0 \\ 0 & 0 & 0 & 0 & 0 & 0 & -R_D & 0 \\ 0 & 0 & 0 & 0 & 0 & 0 & 0 & -R_Q \end{bmatrix} \nabla H(x) + Gu$$

$$y = G^T \nabla H(x) = \begin{bmatrix} \omega \\ I_d \\ I_q \\ I_f \end{bmatrix}, \; G^T = \begin{bmatrix} 0 & 1 & 0 & 0 & 0 & 0 & 0 & 0 \\ 0 & 0 & 1 & 0 & 0 & 0 & 0 & 0 \\ 0 & 0 & 0 & 1 & 0 & 0 & 0 & 0 \\ 0 & 0 & 0 & 0 & 1 & 0 & 0 & 0 \end{bmatrix}, \; u = \begin{bmatrix} \tau \\ V_d \\ V_q \\ V_f \end{bmatrix} \tag{3.5}$$

where the Hamiltonian is given by the sum of the electrical and mechanical energy:

$$\begin{aligned} H(x) &= H_d(x) + H_q(x) + H_m(x) \\ &= \begin{bmatrix} \Psi_d \\ \Psi_f \\ \Psi_D \end{bmatrix}^T \begin{bmatrix} L_d & \kappa M_f & \kappa M_D \\ \kappa M_f & L_f & L_{fD} \\ \kappa M_D & L_{fD} & L_D \end{bmatrix}^{-1} \begin{bmatrix} \Psi_d \\ \Psi_f \\ \Psi_D \end{bmatrix} \\ &\quad + \begin{bmatrix} \Psi_q \\ \Psi_g \\ \Psi_Q \end{bmatrix}^T \begin{bmatrix} L_q & \kappa M_g & \kappa M_Q \\ \kappa M_g & L_g & L_{gQ} \\ \kappa M_Q & L_{gQ} & L_Q \end{bmatrix}^{-1} \begin{bmatrix} \Psi_q \\ \Psi_g \\ \Psi_Q \end{bmatrix} + J^{-1}p^2. \end{aligned}$$

Here the power-pairs $(V_d, I_d), (V_q, I_q)$ correspond to the external electrical power supplied by the generator. In addition, the power-pair $(V_f, I_f)$ corresponds to the power supplied by the exciter to the synchronous machine. Finally, the pair $(\tau, \omega)$ is associated with the mechanical power injected into the synchronous machine. As noted from the port-Hamiltonian structure of the system (3.5), it naturally follows that the system is *passive* with respect to the previously mentioned input/output pairs, i.e.

$$\dot{H} \leq \tau\omega + V_d I_d + V_q I_q + V_f I_f.$$

**Remark 3.2** (State-dependent interconnection matrix) A crucial observation is that the interconnection structure of the port-Hamiltonian system (3.5) depends on the state $x$. This property significantly increases the complexity of a Lyapunov based stability analysis of equilibria that are different from the origin, see [2,9,24,25] for more details on this challenge.

## 4. Model reduction of the synchronous machine

To simplify the analysis of (networked) synchronous machines, it is preferable to consider reduced-order models with decreasing complexity [7,8,26]. In this section we, following the exposition of [7], discuss briefly how several well-known lower order models are obtained from the first-principle model (3.1). In each reduction step, the underlying assumptions and validity of the reduced-order model are discussed.

The main assumptions rely on timescale separation implying that singular perturbation techniques can be used to obtain reduced-order models [27]. In particular, in the initial reduction step, this allows the stator windings of the synchronous machine to be considered in quasi-steady state. In [28] this quasi-steady-state assumption is validated by the use of iterative timescale separation. In doing so, it is assumed that the frequency is around the synchronous frequency[3] $\omega_s$ and that $\dot{\Psi}_d, \dot{\Psi}_q$ are assumed to be small [7].

**Assumption 4.1** (Operation around $\omega \approx \omega_s$) The synchronous machine is operating around synchronous frequency ($\omega \approx \omega_s$) and in addition $\dot{\Psi}_d$ and $\dot{\Psi}_q$ are small compared to $-\omega\Psi_q$ and $\omega\Psi_d$ which implies

$$\begin{bmatrix} V_d \\ V_q \end{bmatrix} \approx -\begin{bmatrix} R_s & 0 \\ 0 & R_s \end{bmatrix}\begin{bmatrix} I_d \\ I_q \end{bmatrix} + \omega_s \begin{bmatrix} -\Psi_q \\ \Psi_d \end{bmatrix}. \tag{4.1}$$

**Remark 4.2** (Singular perturbation process) It is known that during transients $\Psi_d, \Psi_q$ oscillate with high frequency equal to $\omega \approx \omega_s$ such that $\dot{\Psi}_d, \dot{\Psi}_q$ become very large. The validation of the contradicting Assumption 4.1 is part of a singular perturbation process where the slow variables are approximated by taking the averaging effect of the fast oscillatory variables [27,28].

By Assumption 4.1, the two differential Equations (3.1c) and (3.1d) corresponding to $\Psi_d, \Psi_q$ are replaced by algebraic Equation (4.1), so that a system of differential-algebraic equations (DAEs) is obtained [7]. For many power system studies, it is desirable to rephrase and simplify the model (3.1f)–(3.1a) together with the algebraic Equation (4.1) so that they are in a more acceptable form and easier to interface to the power system network equations. In the following sections, under some additional assumptions based on timescale separation, we eliminate the two algebraic constraints obtained by putting an equality in Equation (4.1). Before examining how this is done, it is necessary to relate the circuit equations to the flux conditions inside the synchronous machine when it is in the steady state, transient state or the subtransient state.

### 4.1. Distinction of operation states

Following the established literature on power systems [6–8,26], a distinction between three different operation states of the synchronous machine is made. Each of the three

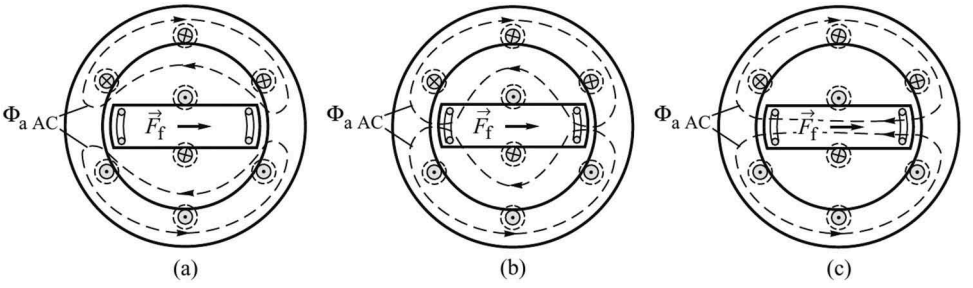


**Figure 2.** The path of the armature flux in: (a) the subtransient state (screening effect of the damper windings and the field winding); (b) the transient state (screening effect of the field and *g*-damper winding only); (c) the steady state [7].

characteristic operation states correspond to different stages of rotor screening and a different timescale [27,28], see Figure 2.

Immediately after a fault, the current induced in both the rotor field and damper windings forces the armature reaction flux completely out of the rotor to keep the rotor flux linkages constant (this is also referred to as the *Lenz effect*), see Figure 2(a), and the generator is said to be in the *subtransient state* [7,8].

As energy is dissipated in the resistance of the rotor windings, the currents maintaining constant rotor flux linkages decay with time allowing flux to enter the windings. As for typical generators the rotor *DQ*-damper winding resistances are the largest, the *DQ*-damper currents are the first to decay, allowing the armature flux to enter the rotor pole face. However, it is still forced out of the field winding and the *g*-damper winding itself, see Figure 2(b). Then, the generator is said to be in the *transient state*.

The field and *g*-winding currents then decay with time to their steady-state values allowing the armature reaction flux eventually to enter the whole rotor and assume the minimum reluctance path. Then, the generator is in *steady state* as illustrated in Figure 2(c) [7].

**Remark 4.3** (Properties of the g-damper winding) Since the field winding and *g*-damper winding resistances are comparable and are typically much smaller compared to the *DQ*-damper winding resistances, the field winding *f* and the *g*-damper winding have similar properties in the different operation states.

### *4.1.1. Synchronous machine parameters*

Depending on which state the synchronous machine is operating in, the effective impedance of the armature coil to any current change will depend on the parameters of the different circuits, their mutual coupling and whether or not the circuits are closed or not [7]. The (positive scalar) inductances and timescales associated with transient and subtransient operation are defined by [7]

$$
\begin{aligned}
L'_d &= L_d - \frac{\kappa^2 M_f^2}{L_f}, \qquad T'_{do} = \frac{L_f}{R_f},\\
L'_q &= L_q - \frac{\kappa^2 M_g^2}{L_g}, \qquad T'_{qo} = \frac{L_g}{R_g},\\
L''_d &= L_d - \kappa^2 \left[\frac{M_f^2 L_D + M_D^2 L_f - 2M_f M_D L_{fD}}{L_f L_D - L_{fD}^2}\right],\\
L''_q &= L_q - \kappa^2 \left[\frac{M_g^2 L_Q + M_Q^2 L_g - 2M_g M_Q L_{gQ}}{L_g L_Q - L_{gQ}^2}\right],\\
T''_{do} &= \frac{1}{R_D}\left(L_D - \frac{L_{fD}^2}{L_f}\right), \quad T''_{qo} = \frac{1}{R_Q}\left(L_Q - \frac{L_{gQ}^2}{L_g}\right).
\end{aligned}
\tag{4.2}
$$

Based on the two-reaction theory of [29], the corresponding $d$- and $q$-axis reactances for steady-state operation ($X_d = \omega_s L_d, X_q = \omega_s L_q$), transient operation ($X'_d = \omega_s L'_d$, $X'_q = \omega_s L'_q$) and subtransient operation ($X''_d = \omega_s L''_d, X''_q = \omega_s L''_q$) are defined.

**Remark 4.4** (Relation between (sub)transient reactances) For realistic synchronous machines it holds that $X_d > X'_d > X''_d > 0$ and $X_q \geq X'_q > X''_q > 0$, where $X_q = X'_q$ holds for a salient-pole synchronous machine (where the $g$-damper winding is absent), see also [7], Table 4.3] and [8], Table 4.2] for typical values of these reactances.

**Definition 4.5** (Saliency) The *(sub)transient saliency* is defined as the difference between the (sub)transient reactances, i.e. $X'_d - X'_q; (X''_d - X''_q)$. We say that the (sub) transient saliency is negligible if $X'_d = X'_q; (X''_d = X''_q)$.

For both transient and subtransient state of the machine, different assumptions can be made to obtain the corresponding (differential) equations of the synchronous machine.

## 4.2. Synchronous machine equations

In this section, we discuss the assumptions for transient and subtransient operation and state their corresponding algebraic and differential equations appearing in the synchronous machine models. More detailed derivations can be found in [7], Chapter 11].

### 4.2.1. Transient operation

In transient operation state, the armature flux has penetrated the damper circuits and the field and $g$ windings screen the rotor body from the armature flux. The damper windings are no more effective ($\dot{\Psi}_D = \dot{\Psi}_Q = 0$) and thus the damper currents are zero.

**Assumption 4.6** (Transient operation) During transient operation $I_D = I_Q = 0$.

From Equations (3.2) and (3.3), we can express $\Psi_d, \Psi_q$ can be expressed in terms of $I_d, \Psi_f$ and $I_q, \Psi_g$, respectively. In this way, we obtain the following relationship between the internal (transient) and external emfs given by

$$
V_q = -R_s I_q + X'_d I_d + E'_q \tag{4.3}
$$

$$V_d = -R_s I_d - X'_q I_q + E'_d \tag{4.4}$$

where the internal emfs $E'_q, E'_d$ are defined as $E'_q := \omega_s \left(\frac{\kappa M_f}{L_f}\right) \Psi_f$ and $E'_d := -\omega_s \left(\frac{\kappa M_g}{L_g}\right) \Psi_g$. However, the flux linkages $\Psi_f, \Psi_g$ do not remain constant during transient operation but change slowly as the armature flux penetrates through the windings [7]. By substituting Equations (3.1f) and (3.1g), the differential equations for $E'_q, E'_d$ are derived as

$$\dot{E}'_q = \frac{E_f + (X_d - X'_d) I_d - E'_q}{T'_{do}} \tag{4.5}$$

$$\dot{E}'_d = \frac{-(X_q - X'_q) I_q - E'_d}{T'_{qo}}. \tag{4.6}$$

where we used that $I_D = I_Q = 0, T'_{do} = L_f / R_f, T'_{qo} = L_g / R_g$ and the definition $E_f := \omega_s \kappa M_f V_f / R_f$ for the scaled excitation voltage.

### 4.2.2. Subtransient operation

During the subtransient period, the rotor damper coils screen both the field winding and the rotor body from changes in the armature flux. The field and $g$ flux linkages $\Psi_f, \Psi_g$ remain constant during this period while the damper winding flux linkages decay with time as the generator moves towards the transient state [7]. Therefore, we make here a different assumption compared to Section 4.2.1.

**Assumption 4.7** (Subtransient operation) During subtransient operation the flux linkages $\Psi_f, \Psi_g$ are constant.

Using Equation (3.2) we can express $\Psi_d$ in terms of $i_d, \Psi_f, \Psi_D$. Similarly, using Equation (3.3) one can express $\Psi_d$ in terms of $i_d, \Psi_f, \Psi_D$:

$$\Psi_d = L''_d I_d + k_1 \Psi_f + k_2 \Psi_D,$$

$$\Psi_q = L''_q I_q + k_3 \Psi_g + k_4 \Psi_Q,$$

where

$$k_1 = \kappa \cdot \frac{M_f L_D - M_D L_{fD}}{L_f L_D - L_{fD}^2}, \qquad k_2 = \kappa \cdot \frac{M_D L_f - M_f L_{fD}}{L_f L_D - L_{fD}^2},$$

$$k_3 = \kappa \cdot \frac{M_g L_Q - M_Q L_{gQ}}{L_g L_Q - L_{gQ}^2}, \qquad k_4 = \kappa \cdot \frac{M_Q L_g - M_g L_{gQ}}{L_g L_Q - L_{gQ}^2}$$

Together with Assumption 4.1, we obtain

$$V_q = -R_s I_q + X''_d I_d + E''_q \tag{4.7}$$

$$V_d = -R_s I_d - X''_q I_q + E''_d \tag{4.8}$$

where the subtransient emfs are defined as

$$E''_q := \omega_s(k_1\Psi_f + k_2\Psi_D)$$

$$E''_d := -\omega_s(k_3\Psi_g + k_4\Psi_Q) \tag{4.9}$$

Using Assumption 4.7, and by eliminating the $I_f, \Psi_d$ from (Equation (3.2) and $I_g, \Psi_q$ from (Equation (3.3) we obtain, respectively, the differential equations of $E''_q$ and $E''_d$:

$$T''_{do}\dot{E}''_q = E'_q - E''_q + (X'_d - X''_d)I_d, \tag{4.10}$$

$$T''_{qo}\dot{E}''_d = E'_d - E''_d - (X'_q - X''_q)I_q. \tag{4.11}$$

### 4.2.3. Frequency dynamics

Recall that the frequency dynamics of the full-order model is described by Equation (3.1b):

$$J\dot{\omega} = \Psi_q I_d - \Psi_d I_q - d\omega + \tau. \tag{4.12}$$

Since the mechanical damping force $F_d = -d\omega$ is often very small in large machines, it is neglected in many synchronous machine models [7,8].

**Assumption 4.8** (Negligible mechanical damping) The mechanical damping of the synchronous machine is negligible, i.e. $d = 0$.

It is convenient to express the frequency dynamics in terms of the *frequency deviation* $\Delta\omega := \omega - \omega_s$ with respect to the synchronous frequency $\omega_s$. By using Assumptions 4.1, 4.8 the dynamics of the frequency deviation is governed by

$$M\Delta\dot{\omega} = -\underbrace{\left(V_d I_d + V_q I_q + R_s(I_d^2 + I_q^2)\right)}_{P_e} + \underbrace{\omega_s\tau}_{P_m} = -P_e + P_m. \tag{4.13}$$

Here it is common practice to multiply Equation (4.12) by the synchronous frequency $\omega_s$ and to define the quantity $M := \omega_s J$ . Here $P_m$ is the mechanical power injection and $P_e$ is the electrical power produced by the synchronous generator.

**Remark 4.9** (Alternative formulation of frequency dynamics) Note that by Equations (4.7) and (4.8) the electrical power $P_e$ produced by the synchronous generator alternatively takes the form

$$P_e = E''_d I_d + E''_q I_q + (X''_d - X''_q)I_d I_q \tag{4.14}$$

such that the differential Equation (4.14) can be rewritten as

$$M\Delta\dot{\omega} = -E''_d I_d - E''_q I_q - (X''_d - X''_q)I_d I_q + P_m. \tag{4.15}$$

### 4.3. Synchronous machine models

Based on the results established in Section 4.2, several generator models with decreasing complexity and accuracy are developed. In each model reduction step, the validity and assumptions made in the corresponding model are discussed.

#### 4.3.1. Sixth-order model

By combining the equations derived in Section 4.2, a sixth-order model describing the synchronous generator is obtained. In particular, by Equations (4.5), (4.6), (4.11), (4.12) and (4.16) we obtain the following system of ordinary differential equations describing the generator dynamics [7]:

$$\dot{\delta} = \Delta\omega \tag{4.16a}$$

$$M\Delta\dot{\omega} = P_m - E''_d I_d - E''_q I_q - (X''_d - X''_q) I_d I_q \tag{4.16b}$$

$$T'_{do}\dot{E}'_q = E_f - E'_q + I_d(X_d - X'_d) \tag{4.16c}$$

$$T'_{qo}\dot{E}'_d = -E'_d - I_q(X_q - X'_q) \tag{4.16d}$$

$$T''_{do}\dot{E}''_q = E'_q - E''_q + I_d(X'_d - X''_d) \tag{4.16e}$$

$$T''_{qo}\dot{E}''_d = E'_d - E''_d - I_q(X'_q - X''_q), \tag{4.16f}$$

where $\delta(t) := \gamma(t) - \omega_s t$ represents the rotor angle with respect to the synchronous rotating reference frame. By Equations (4.7) and (4.8) the internal and external voltages of the synchronous generator are related by

$$\begin{bmatrix} V_d \\ V_q \end{bmatrix} = \begin{bmatrix} E''_d \\ E''_q \end{bmatrix} - \begin{bmatrix} R_s & X''_q \\ -X''_d & R_s \end{bmatrix} \begin{bmatrix} I_d \\ I_q \end{bmatrix}. \tag{4.17}$$

It is worth noting the similar structure of these (differential) equations. Equation (4.17) and the right-hand side of Equations (4.16c)–(4.16f) relates to the equivalent $d$- or $q$-axis generator circuits, with the resistances neglected, as shown in Figure 3. In particular, the algebraic Equation (4.17) corresponds to the right-hand side of Figure 3. In addition, the subtransient dynamics Equations (4.16e), (4.16f) corresponds to the centre reactances $X'_d - X''_d, X'_q - X''_q$ illustrated in Figure 3 and the transient dynamics Equations (4.16c) and (4.16d) correspond to the left-hand side of Figure 3. Observe that there is no additional voltage in the $q$-axis due to the absence of a field winding on this axis.

#### 4.3.2. Fifth-order model

In a salient-pole generator, the laminated rotor construction prevents eddy currents flowing in the rotor body such that there is no screening in the $q$-axis implying that $X_q = X'_q$ [7]. In that case, the $g$-winding is absent in the full-order model (1). Consequently, $E_{d'}$ is absent so that the fifth-order model becomes

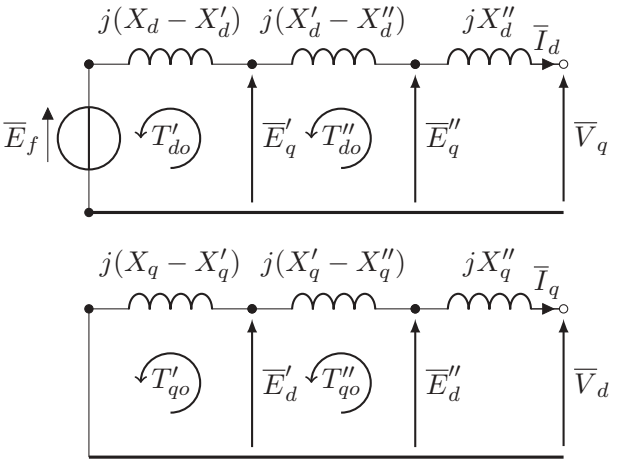


**Figure 3.** The generator equivalent circuits for both *dq*-axes in case the stator winding resistance $R_s$ is neglected [7].

$$\begin{aligned}
\dot{\delta} &= \Delta\omega \\
M\Delta\dot{\omega} &= P_m - E''_d I_d - E''_q I_q - (X''_d - X''_q) I_d I_q \\
T'_{do}\dot{E}'_q &= E_f - E'_q + I_d(X_d - X'_d) \\
T''_{do}\dot{E}''_q &= E'_q - E''_q + I_d(X''_d - X''_d) \\
T''_{qo}\dot{E}''_d &= -E''_d - I_q(X'_q - X''_q).
\end{aligned} \tag{4.18}$$

### 4.3.3. Fourth-order model

In this model, the subtransient dynamics of the sixth-order model induced by the damper windings is neglected. This is motivated by the fact that $T''_{do} \ll T'_{do}, T''_{qo} \ll T'_{qo}$. Therefore, the dynamics corresponding with $E''_q, E''_d$ is at a much faster timescale compared to the $E'_q, E'_d$ dynamics. As a result, at the slower timescale we obtain the quasi-steady-state condition [27]:

$$\begin{aligned}
E''_q &= E'_q + I_d(X'_d - X''_d) \\
E''_d &= E'_d - I_q(X'_q - X''_q).
\end{aligned} \tag{4.19}$$

Substitution of the latter algebraic equations in the remaining four differential equations yields the fourth-order model

$$\begin{aligned}
\dot{\delta} &= \Delta\omega \\
M\Delta\dot{\omega} &= P_m - D\Delta\omega - E_{d'} I_d - E_{q'} I_q - (X'_d - X'_q) I_d I_q \\
T'_{do}\dot{E}'_q &= E_f - E'_q + I_d(X_d - X'_d) \\
T'_{qo}\dot{E}_d &= -E'_d - I_q(X_q - X'_q).
\end{aligned} \tag{4.20}$$

**Remark 4.10** (Transient operation) Note that Equation (4.19) together with Equation (4.17) also implies Equations (4.3) and (4.4) as expected since the subtransient dynamics is neglected.

As the damper windings are ignored, the air-gap power appearing in the frequency dynamics neglects the asynchronous torque produced by the damper windings. To compensate the effects of the damper windings typically a linear asynchronous damping power $D\Delta\omega$ with damping constant $D>0$ is introduced. However, more accurate non-linear approximations of the damping power exist as well, see [7], Chapter 5.2].

#### 4.3.4. Third-order model

Starting from the fourth-order model, we make here the same assumptions as done in the transition from the sixth-order model to the fifth-order model (no $E'_d$) so that the third-order model, which also referred to as the *flux-decay model* or *one-axis model* [8], is given by

$$\dot{\delta} = \Delta\omega \tag{4.21a}$$

$$M\Delta\dot{\omega} = -D\Delta\omega + P_m - E'_q I_q - (X'_d - X'_q) I_d I_q \tag{4.21b}$$

$$T'_{do}\dot{E}'_q = E_f - E'_q + I_d(X_d - X'_d). \tag{4.21c}$$

#### 4.3.5. Second-order classical model

The second-order model is derived from the fourth-order (or third-order) model by assuming that the internal emfs $E'_q, E'_d$ are constant [6–8]. This can be validated if the timescales $T'_{qo}, T'_{do}$ are large (of the order of a few seconds) so that the internal emfs $E'_q, E'_d$ can be approximated by a constant (on a bounded time interval) provided that $E_f, I_d, I_q$ do not change much. From this assumption, a constant voltage behind the transient reactance model is obtained which is commonly referred to as the *constant flux linkage model* or *classical model* [6–8]:

$$\begin{aligned} \dot{\delta} &= \Delta\omega \\ M\Delta\dot{\omega} &= -D\Delta\omega + P_m - E'_q I_q - E'_d I_d - (X'_d - X'_q) I_d I_q \end{aligned} \tag{4.22}$$

The assumption that the changes in $dq$-currents and the internal emfs are small implies that only generators located a long way from the point of the disturbance should be represented by the classical model [7]. In addition, since the assumption that $E'_q, E'_q$ is constant is only valid on a limited time-interval, the classical model is only valid for analyzing the *first swing stability* [6]. Indeed, in for example [21] it was shown that the second-order swing Equation (4.22) is not valid for asymptotic stability analyses.

## 5. Multi-machine models

To obtain a representation of the power grid, we consider a multi-machine network. For simplicity, we consider the case that each node in the network represents a synchronous machine, that is, each node represents either a synchronous generator, or a synchronous motor. In addition, we assume that the stator winding resistances and the resistances in the network are negligible. This assumption is valid for networks with high voltage transmission lines where the line resistances are negligible.

**Assumption 5.1** (Inductive lines and $R_s = 0$) The network is considered to be purely inductive and the stator winding resistances are negligible, i.e. $R_s = 0$.

In this section, the multi-machine models starting from the sixth-, third-, and second-order models for the synchronous generator are established. The derivations of the fourth- and fifth-order multi-machine models are omitted as these are very similar to ones presented in this section. To obtain reduced-order multi-machine models, the equations for the nodal currents in the network are derived which are then substituted in the single generator models reformulated in Section 4.3.

### 5.1. Sixth-order multi-machine model

For the sixth- (and fifth-)order model(s), it is convenient to make the following assumption which is valid for synchronous generators with damper windings in both $d$- and $q$-axes [7].

**Assumption 5.2** ($X''_{di} = X''_{qi}$) For each synchronous machine in the network, the subtransient saliency is negligible, i.e. $X''_{di} = X''_{qi}\ \forall i \in \mathcal{V}$.

By Assumption 5.2, the second term of the electrical power Equation (4.14) appearing in the frequency dynamics (4.16b) vanishes. Moreover, the assumption of $X''_d = X''_q$ allows the two individual $d$- and $q$-axis circuits in Figure 3 to be replaced by one equivalent circuit, see Figure 4. As a result, all the voltages, emfs and currents are phasors in the synchronous rotating reference frame of rather than their components resolved along the $d$- and $q$-axes. An important advantage of this is that the generator reactance may be treated in a similar way as the reactance of a transmission line, as we will show later. This has particular importance for multi-machine systems when combining the algebraic equations describing the generators and the network [7].

As illustrated in Figure 4, the internal and external voltages are related to each other by

$$\bar{E}''_i = \bar{V}_i + jX''_{di}\bar{I}_i, \qquad \forall i \in \mathcal{V}. \tag{5.1}$$

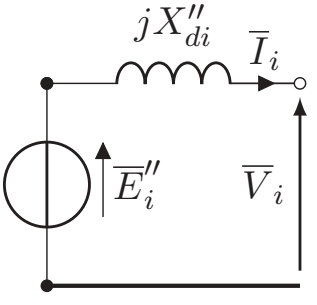


**Figure 4.** Subtransient emf behind a subtransient reactance.

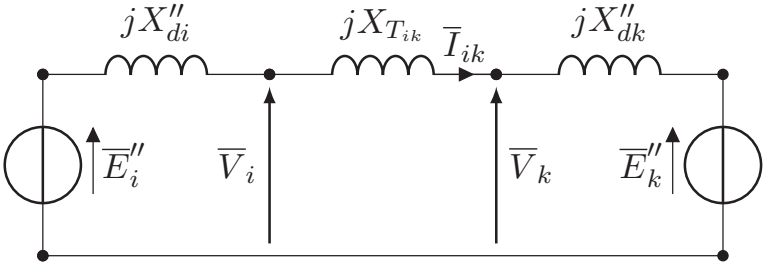


**Figure 5.** Interconnection of two synchronous machines governed by the fifth- or sixth-order model by a purely inductive transmission line with reactance $X_{T_{ik}}$.

Consider a power network where each node $i \in \mathcal{V} = \{1, 2, \ldots, n\}$ represents a synchronous machine and each edge $(i, k) \in \mathcal{E}$ a transmission line, see Figure 5 for a two-node case.

To derive the algebraic equations associated with the network, we assume that the network operates at steady state. Under this assumption, the network equations take the form

$$\bar{I}_s = Y\bar{V}_S = Y\bar{E}''_S$$

where $\bar{I}_s, \bar{V}_s, \bar{E}''_s \in \mathbb{C}^n$ represent the nodal current and external/internal voltage phasors with respect to the synchronous rotating reference frame and $Y \in \mathbb{C}^{n\times n}$ is the admittance matrix of the network. The admittance matrix $\mathcal{Y} \in \mathbb{C}^{n\times n}$ is obtained by adding the reactances $X''_{di}, i \in \mathcal{V}$ to the transmission line reactances, i.e. $\mathcal{Y}$ takes the form $\mathcal{Y}_{ii} = G_{ii} + jB_{ii}, \mathcal{Y}_{ik} = -G_{ik} - jB_{ik}, i \neq k$ where the susceptances are given by [23]

$$\begin{aligned} B_{ik} &= \begin{cases} 0 & \text{if nodes and } k \text{ are not connected} \\ -\frac{1}{X_{ik}} & \text{if nodes and } k \text{ are connected} \end{cases} \\ B_{ii} &= \sum_{k\in\mathcal{N}_i} B_{ik} \end{aligned} \tag{5.2}$$

and where $X_{ik} := X_{T_{ik}} + X''_{di} + X''_{dk}$ is the total reactance between the subtransient voltage sources as illustrated in Figure 5. As we assumed purely inductive lines, see Assumption 5.1, the conductance matrix equals the zero matrix and thus $G_{ik} = 0\ \forall i, k \in \mathcal{V}$. We note that in the derivations in Section 4 the currents $\bar{I} = V_q + jV_d$ and internal voltages $\bar{E}'' = E''_q + jE''_d$ are expressed with respect to the *local* $dq0$-reference frame of the synchronous machine. Thus, according to Equation (2.3), $\bar{I}_s = \mathrm{diag}(e^{-j(\omega_s t-\gamma_i)})\bar{I} = \mathrm{diag}(e^{j\delta_i})\bar{I}$ and similarly $\bar{E}''_s = \mathrm{diag}(e^{j\delta_i})\bar{E}''$. Consequently,

$$\bar{I} = \mathrm{diag}(e^{-j\delta_i})\mathcal{Y}\,\mathrm{diag}(e^{j\delta_i})\bar{E}'', \tag{5.3}$$

where $\bar{I} = \mathrm{col}(\bar{I}_1, \ldots, \bar{I}_n), \bar{E}'' = \mathrm{col}(\bar{E}''_1, \ldots, \bar{E}''_n)$. Then, the $dq$-current phasor at node $i$ takes the form

$$\bar{I}_i = \mathcal{Y}_{ii}\bar{E}_i'' + \sum_{k\in\mathcal{N}_i} \mathcal{Y}_{ik} e^{-j\delta_{ik}} \bar{E}_k''. \tag{5.4}$$

Using the phasor representation $\bar{E}_i'' = E_{qi}'' + jE_{di}''$, $\bar{I}_i = I_{qi} + jI_{di}$, and equating both the real and imaginary part of Equation (5.4), we obtain after rewriting

$$\begin{aligned} I_{di} &= B_{ii}E_{qi}'' - \sum_{k\in\mathcal{N}_i}\Big[B_{ik}(E_{dk}'' \sin\delta_{ik} + E_{qk}'' \cos\delta_{ik})\Big], \\ I_{qi} &= -B_{ii}E_{di}'' - \sum_{k\in\mathcal{N}_i}\Big[B_{ik}(E_{qk}'' \sin\delta_{ik} - E_{dk}'' \cos\delta_{ik})\Big]. \end{aligned} \tag{5.5}$$

**Remark 5.3** (Nonzero transfer conductances) Compared to (5.5), a slightly more complicated expression for the $dq$-currents can be derived in the more general case where the transfer conductances are nonzero, see e.g. [23].

By substituting the network Equation (5.5) into the sixth-order model of the synchronous machine derived in Section 4.3.1, the multi-machine model Equation (5.6) is obtained. A subscript $i$ is added to the model Equation (4.16) to indicate that this is the model of the synchronous machine $i \in \mathcal{V}$.

$$\begin{aligned} \dot{\delta}_i &= \Delta\omega_i \\ M_i\Delta\dot{\omega}_i &= P_{mi} + \sum_{k\in\mathcal{N}_i} B_{ik}\big[(E_{di}''E_{dk}'' + E_{qi}''E_{qk}'')\sin\delta_{ik} + (E_{di}''E_{qk}'' - E_{qi}''E_{dk}'')\cos\delta_{ik}\big] \\ T_{doi}'\dot{E}_{qi}' &= E_{fi} - E_{qi}' + (X_{di} - X_{di}')\left(B_{ii}E_{qi}'' - \sum_{k\in\mathcal{N}_i}\big[B_{ik}(E_{dk}''\sin\delta_{ik} + E_{qk}''\cos\delta_{ik})\big]\right) \\ T_{qoi}'\dot{E}_{di}' &= -E_{di}' + (X_{qi} - X_{qi}')\left(B_{ii}E_{di}'' - \sum_{k\in\mathcal{N}_i}\big[B_{ik}(E_{dk}''\cos\delta_{ik} - E_{qk}''\sin\delta_{ik})\big]\right) \\ T_{doi}''\dot{E}_{qi}'' &= E_{qi}' - E_{qi}'' + (X_{di}' - X_{di}'')\left(B_{ii}E_{qi}'' - \sum_{k\in\mathcal{N}_i}\big[B_{ik}(E_{dk}''\sin\delta_{ik} + E_{qk}''\cos\delta_{ik})\big]\right) \\ T_{qoi}''\dot{E}_{di}'' &= E_{di}' - E_{di}'' + (X_{qi}' - X_{qi}'')\left(B_{ii}E_{di}'' - \sum_{k\in\mathcal{N}_i}\big[B_{ik}(E_{dk}''\cos\delta_{ik} - E_{qk}''\sin\delta_{ik})\big]\right) \end{aligned} \tag{5.6}$$

The electrical power $P_{ei}$ produced by synchronous machine $i$ is obtained from Equations (4.14) and (5.5), and is given by

$$\begin{aligned} P_{ei} &= E_{di}''I_{di} + E_{qi}''I_{qi} \\ &= \sum_{k\in\mathcal{N}_i} \underbrace{-B_{ik}\big[(E_{di}''E_{dk}'' + E_{qi}''E_{qk}'')\sin\delta_{ik} + (E_{di}''E_{qk}'' - E_{qi}''E_{dk}'')\cos\delta_{ik}\big]}_{P_{ik}}. \end{aligned} \tag{5.7}$$

**Remark 5.4** (Energy conservation) Since the transmission lines are purely inductive by assumption, there are no energy losses in the transmission lines implying that the following energy conservation law holds: $P_{ik} = -P_{ki}$ where $P_{ik}$ given in Equation (5.7) represents the power transmission from node $i$ to node $k$. In particular, we also have $\sum_{i\in\mathcal{V}} P_{ei} = 0$ with $P_{ei}$ is given by Equation (5.7).

**Remark 5.5** (Including resistances) While in the above model the resistances of the network and the stator windings are neglected, the model easily extends to the case of nonzero resistances. This can be done following the same procedure as before but instead substituting the more complicated expression for the currents $I_{di}, I_{qi}$, see Remark 5.3.

### 5.2. Third-order multi-machine model

The derivation of the third-order multi-machine models proceeds along the same lines as for the sixth-order model. For similar reasons as for the sixth- and fifth-order models, it is convenient for the second-, third-, and fourth-order multi-machine models to assume that the transient saliency is negligible.

**Assumption 5.6** ($X'_{di} = X'_{qi}$) The transient saliency is negligible: $X'_{di} = X'_{qi}\ \forall i \in \mathcal{V}$.

By making the *classical assumption* that $X'_d = X'_q$, the second term of the electrical power appearing in the frequency dynamics Equation (4.21b) vanishes [7]. In addition, the assumption of $X'_d = X'_q$ allows the separate $d$- and $q$-axis circuits shown in Figure 3 to be replaced by one simple equivalent circuit, see Figure 6, representing a transient voltage source behind a transient reactance.

**Remark 5.7** (Negligible transient saliency) Although there is always some degree of transient saliency implying that $X'_{di} \neq X'_{qi}$, it should be noted that if the network reactances are relatively large, then the effect of the transient saliency on the power network dynamics is negligible making Assumption 5.6 acceptable [7].

Similar as before, the interconnection of two synchronous machines can be represented as in Figure 7.

As illustrated in this figure, the internal and external voltages are related to each other by [7]

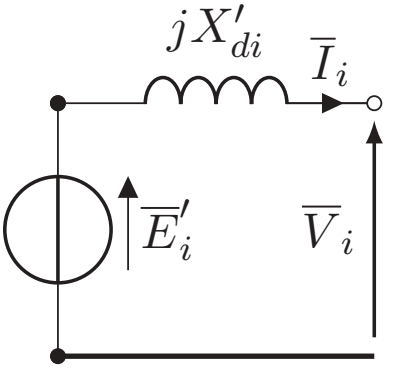


**Figure 6.** Single generator equivalent circuit in case the transient saliency is neglected [7].

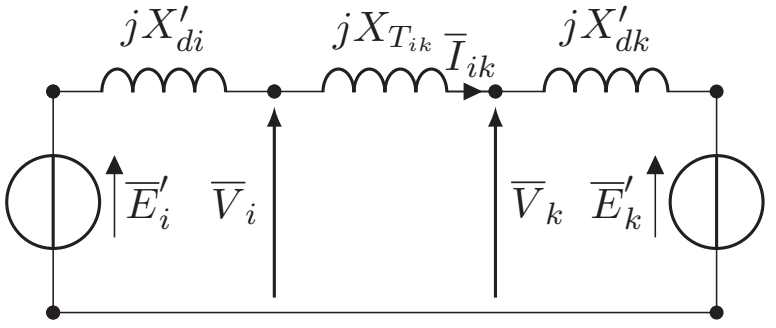


**Figure 7.** Interconnection of two synchronous machines governed by the second-, third-, or fourth-order model by a purely inductive transmission line with reactance $X_{T_{ik}}$.

$$\bar{E}'_i = \bar{V}_i + jX'_{di}\bar{I}_i, \qquad \forall i \in \mathcal{V}. \tag{5.8}$$

The algebraic equations associated with the network amount to [23]

$$\bar{I} = \operatorname{diag}(e^{-j\delta_i})\mathcal{Y}\operatorname{diag}(e^{j\delta_i})\bar{E}', \tag{5.9}$$

resulting in a similar expression for the $dq$-currents as for the sixth-order model:

$$\begin{aligned} I_{di} &= B_{ii}E'_{qi} - \sum_{k\in\mathcal{N}_i}\left[B_{ik}(E'_{dk}\sin\delta_{ik} + E'_{qk}\cos\delta_{ik})\right], \\ I_{qi} &= -B_{ii}E'_{di} - \sum_{k\in\mathcal{N}_i}\left[B_{ik}(E'_{qk}\sin\delta_{ik} - E'_{dk}\cos\delta_{ik})\right]. \end{aligned} \tag{5.10}$$

**Remark 5.8** (Susceptance matrix for 4th,3rd and 2nd-order models) Note that in contrast to the 6th and 5th-order models, for the 4rd, 3rd and 2nd-order model the susceptances satisfy $B_{ik} = -\frac{1}{X_{ik}}$, for all $(i,k) \in \mathcal{E}$ where $X_{ik} := X_{T_{ik}} + X'_{di} + X'_{dk}$ is the total reactance between the transient voltage sources as illustrated in Figure 7.

By using the third-order model of the synchronous machine (4.21), the network Equation (5.10), and the fact that $E_{di}{}' = 0$ for the third-order model, the flux-decay (or one-axis) multi-machine model is obtained.

$$\begin{aligned} \dot{\delta}_i &= \Delta\omega_i \\ M_i\Delta\dot{\omega}_i &= P_{mi} - D_i\Delta\omega_i + \sum_{k\in\mathcal{N}_i} B_{ik}E'_{qi}E'_{qk}\sin\delta_{ik} \\ T'_{doi}\dot{E}'_{qi} &= E_{fi} - E'_{qi} + (X_{di} - X'_{di})(B_{ii}E'_{qi} - \sum_{k\in\mathcal{N}_i} B_{ik}E'_{qk}\cos\delta_{ik})) \end{aligned} \tag{5.11}$$

It is observed that similar to the sixth-order multi-machine model (5.6), Remark 5.4 and Remark 5.5 also hold for the third-order model (5.11).

### 5.3. The classical multi-machine network

The derivation of the classical second-order swing equations takes a slightly different approach compared to the multi-machine models obtained previously. Suppose that Assumption 5.6 holds. Let the transient voltage phasor be represented as $\bar{E}'_i = e^{j\alpha_i}|\bar{E}'_i|$, then by Equation (5.9) we have

$$\bar{I}_i = \mathcal{Y}_{ii} e^{j\alpha_i} \left|\bar{E}'_i\right| + \sum_{k \in \mathcal{N}_i} \mathcal{Y}_{ik} e^{-j\delta_{ik}} e^{j\alpha_k} \left|\bar{E}'_k\right|, \quad \forall i \in \mathcal{V}.$$

By defining the angles[4] $\theta_i := \delta_i + \alpha_i$ it can be shown that the electrical power supplied by the synchronous machine amounts to

$$\begin{aligned} P_{ei} &= \Re(\bar{E}'_i \bar{I}_i^*) = \Re(\bar{E}_i'^* \bar{I}_i) = \Re(\mathcal{Y}_{ii} |\bar{E}'_i|^2 + \sum_{k \in \mathcal{N}_i} \mathcal{Y}_{ik} e^{-j(\delta_{ik} + \alpha_{ik})} \left|\bar{E}'_i\right| \left|\bar{E}'_k\right|) \\ &= -\sum_{k \in \mathcal{N}_i} B_{ik} \sin \theta_{ik} \left|\bar{E}'_i\right| \left|\bar{E}'_k\right|. \end{aligned}$$

It is convenient to express the system dynamics in terms of the voltage angles $\theta_i$. By noting that $\alpha_i$ is constant[5] it follows that $\dot{\theta}_i = \dot{\delta}_i = \Delta\omega_i$. Hence, the multi-machine classical model is described by the well-known *swing equations*

$$\begin{aligned} \dot{\theta}_i &= \Delta\omega_i \\ M_i \Delta\dot{\omega}_i &= -D_i \Delta\omega_i + P_{mi} + \sum_{k \in \mathcal{N}_i} B_{ik} \sin \theta_{ik} \left|\bar{E}'_i\right| \left|\bar{E}'_k\right|, \qquad i \in \mathcal{V}. \end{aligned} \tag{5.12}$$

**Remark 5.9** (Load nodes) In the multi-machine models constructed in this section it is assumed that each node in the network represents a synchronous machine. However, a more realistic model of a power network can be obtained by making a distinction between generator and load nodes [30,31]. This is beyond the scope of the present article. Instead, we assume that some synchronous machines act as synchronous motors for which the injected mechanical power is negative.

## 6. Energy functions

When analyzing the stability of a synchronous machine (or a multi-machine network) it is desired to search for a suitable Lyapunov function. Often the physical energy stored in the system can be used as a Lyapunov function for the zero-input case. In this section, we derive the energy functions of the reduced order models of the synchronous machine. In addition, the energy functions corresponding to the transmission lines are obtained.

### 6.1. Synchronous machine

The physical energy stored in a synchronous machine consists of both an electrical part and a mechanical part. We first derive the electrical energy of the synchronous machine.

#### 6.1.1. Electrical energy

In this section, we search for an expression for the electrical energy of the reduced order models for the synchronous machine. A natural starting point is to look at the electrical energy of the full-order system and rewrite this in terms of the state variables of the reduced order system. Recall that the electrical energy in the $d$- and $q$-axis of the full-order system is, respectively, given by[6]

$$H_{dq} = H_d + H_q = \begin{bmatrix} \Psi_d \\ \Psi_f \\ \Psi_D \end{bmatrix}^T \begin{bmatrix} L_d & kM_f & kM_D \\ kM_f & L_f & L_{fD} \\ kM_D & L_{fD} & L_D \end{bmatrix}^{-1} \begin{bmatrix} \Psi_d \\ \Psi_f \\ \Psi_D \end{bmatrix} + \begin{bmatrix} \Psi_q \\ \Psi_g \\ \Psi_Q \end{bmatrix}^T \begin{bmatrix} L_q & kM_g & kM_Q \\ kM_g & L_g & L_{gQ} \\ kM_Q & L_{gQ} & L_Q \end{bmatrix}^{-1} \begin{bmatrix} \Psi_q \\ \Psi_g \\ \Psi_Q \end{bmatrix}.$$

Using the definitions of $E'_q, E''_q$ and the reactances $X_d, X'_d, X''_d$ we can express the electrical energy in the $d$-axis as

$$H_d = \frac{1}{2} \begin{bmatrix} \Psi_d \\ E'_q \\ E''_q \end{bmatrix}^T \begin{bmatrix} \frac{\omega_s}{X''_d} & 0 & -\frac{1}{X''_d} \\ 0 & \frac{1}{\omega_s(X_d - X''_d)} + \frac{1}{\omega_s(X'_d - X''_d)} & -\frac{1}{\omega_s(X'_d - X''_d)} \\ -\frac{1}{X''_d} & -\frac{1}{\omega_s(X''_d - X''_d)} & \frac{X_{d'}}{\omega_s(X'_d - X''_d)X''_d} \end{bmatrix} \begin{bmatrix} \Psi_d \\ E'_q \\ E''_q \end{bmatrix} \tag{6.1}$$

and a similar expression for the energy $H_q$ can be derived for the $q$-axis.

**Remark 6.1** (Complexity in derivating:Hdpsid) To obtain (6.1) requires not only computing the inverse of the inductance matrices $\mathcal{L}_d, \mathcal{L}_q$ but also to eliminate the appropriate parameters (such as $L_d, L_q,$ etc.) and variables $(\Psi_f, \Psi_g, \Psi_D, \Psi_Q)$ used in the model (3.1). Interestingly, with the help of the computer algebra program Mathematica 11 we eventually obtain a relatively sparse expression of the electrical energy $H_d$ (and $H_q$) given by Equation (6.1).

*6.1.1.1. Sixth-order model.* We can also express the electrical energy Equation (6.1) in term of the currents $I_d, I_q$ as follows. First, by Assumption 4.1 we eliminate $\Psi_d, \Psi_q$ by substituting $\Psi_q = -\omega_s^{-1}(V_d + R_s I_d), \Psi_d = \omega_s^{-1}(V_q + R_s I_q)$. Then $V_d$, $V_q$ can be eliminated by substituting Equation (4.17), that is, $V_d = E''_d - R_s I_d - X''_q I_q, V_q = E''_q - R_s I_q + X''_d I_d$. Consequently, for the sixth-order model, the electrical energy stored in the machine takes the simpler form

$$H_d = \frac{1}{2\omega_s} \begin{bmatrix} I_d \\ E'_q \\ E''_q \end{bmatrix}^T \begin{bmatrix} X''_d & 0 & 0 \\ 0 & \frac{1}{X_d - X'_d} + \frac{1}{X'_d - X''_d} & -\frac{1}{X'_d - X''_d} \\ 0 & -\frac{1}{X'_d - X''_d} & \frac{1}{X'_d - X''_d} \end{bmatrix} \begin{bmatrix} I_d \\ E'_q \\ E''_q \end{bmatrix}, \tag{6.2}$$

and a similar expression is obtained for the $q$-axis by exchanging the $dq$-subscripts.

**Remark 6.2** (Energy storage in generator circuits) One interesting observation is that Equation (6.2) is identical to the energy stored in the generator equivalent circuits illustrated in Figure 3 in the zero input case ($E_f = 0$). Here we observe that the energy stored in the centre reactances as in Figure 3 is given by

$$\frac{1}{2}LI_d^2 = \frac{1}{2\omega_s}(X'_d - X''_d)I_d^2 = \frac{1}{2\omega_s}(X'_d - X''_d)\left(\frac{1}{X'_d - X''_d}(E'_q - E''_q)\right)^2$$
$$= \frac{1}{2\omega_s}\frac{1}{X'_d - X''_d}\begin{bmatrix} E'_q & E''_q \end{bmatrix}\begin{bmatrix} 1 & -1 \\ -1 & 1 \end{bmatrix}\begin{bmatrix} E'_q \\ E''_q \end{bmatrix}. \tag{6.3}$$

*6.1.1.2. Fifth-order model.* For the fifth-order model, we have that $E'_d = 0$ implying that the electrical energy in the $q$-axis modifies to

$$H_q = \frac{1}{2\omega_s}\begin{bmatrix} I_q \\ E''_d \end{bmatrix}^T \begin{bmatrix} X''_q & 0 \\ 0 & \frac{1}{X'_q - X''_q} \end{bmatrix}\begin{bmatrix} I_q \\ E''_d \end{bmatrix}, \tag{6.4}$$

while the expression for $H_d$ remains identical to the one for the sixth-order model, see Equation (6.2).

*6.1.1.3. Lower-order models.* Since for the fourth-, third- and second-order model the subtransient dynamics is neglected, we can substitute Equation (4.19) into (6.2) such that the electrical energy $H_{dq} := H_d + H_q$ can be written as

$$H_{dq} = \frac{1}{2\omega_s}\begin{bmatrix} I_d \\ E'_q \end{bmatrix}^T \begin{bmatrix} X'_d & 0 \\ 0 & \frac{1}{X_d - X'_d} \end{bmatrix}\begin{bmatrix} I_d \\ E'_q \end{bmatrix} + \frac{1}{2\omega_s}\begin{bmatrix} I_q \\ E'_d \end{bmatrix}^T \begin{bmatrix} X'_q & 0 \\ 0 & \frac{1}{X_q - X'_q} \end{bmatrix}\begin{bmatrix} I_q \\ E'_d \end{bmatrix} \tag{6.5}$$

and for the third-order model we have $E'_d = 0$.

**Remark 6.3** (Synchronous machines reactances as part of line reactances) If the (sub) transient saliency is neglected then the reactance $X'_d\,(X''_d)$ can considered as part the (transmission) network, see Section 5. Therefore, the energy stored in this reactance will be part of the energy stored in the transmission lines which will be discussed in Section 6.2. As a result, the part of the energy Equation (6.5) corresponding with $I_d, I_q$ can be disregarded here. For example, for the fourth-, third- and second-order model the energy function associated to the electrical energy stored in the generator circuit is given by

$$H_{dq} = \frac{1}{2\omega_s}\frac{{E'_q}^2}{X_d - X'_d} + \frac{1}{2\omega_s}\frac{{E'_d}^2}{X_q - X'_q}, \tag{6.6}$$

where $E'_d = 0$ for the third-order model.

Bearing in mind Remark 6.3 and noting that for the second-order model the voltages $E'_q, E'_d$ are constant, it follows that the electrical energy Equation (6.6) is constant as well.

### 6.1.2. Mechanical energy

The rotational kinetic energy of the synchronous machine is given by

$$H_m = \frac{1}{2}J\omega^2 = \frac{1}{2\omega_s}M^{-1}(\Delta\omega + \omega_s)^2 \tag{6.7}$$

where we recall that $M$ is defined as $M = \omega_s J$ as discussed in Section 4.2.3.

## 6.2. Inductive transmission lines

### 6.2.1. Sixth- and fifth-order models

Consider an inductive transmission line between nodes $i$ and $k$ at steady state, see Figure 8.

When expressed in the local $dq$-reference frame of synchronous machine $i$, we observe from Figure 8 that

$$jX_{ik}\bar{I}_{ik} = \bar{E}''_i - e^{-j\delta_{ik}}\bar{E}''_k. \tag{6.8}$$

By equating the real and imaginary part of (6.8) we obtain

$$X_{ik}\begin{bmatrix} I_{qik} \\ -I_{dik} \end{bmatrix} = \begin{bmatrix} E''_{di} - E''_{dk}\cos\delta_{ik} + E''_{qk}\sin\delta_{ik} \\ E''_{qi} - E''_{dk}\sin\delta_{ik} - E''_{qk}\cos\delta_{ik} \end{bmatrix}. \tag{6.9}$$

Note that the energy of the inductive transmission line between nodes $i$ and $k$ is given by

$$H_{ik} = \frac{1}{2}L_{ik}\bar{I}^*_{ik}\bar{I}_{ik} = \frac{X_{ik}}{2\omega_s}(I^2_{dik} + I^2_{qik})$$

which by Equation (6.9) can be written as

$$\begin{aligned} H_{ik} \quad &= -\tfrac{B_{ik}}{\omega_s}\left[\left(E''_{di}E''_{qk} - E''_{dk}E''_{qi}\right)\sin\delta_{ik} - \left(E''_{di}E''_{dk} + E''_{qi}E''_{qk}\right)\cos\delta_{ik}\right. \\ &\left. + \tfrac{1}{2}{E''_{di}}^2 + \tfrac{1}{2}{E''_{dk}}^2 + \tfrac{1}{2}{E''_{qi}}^2 + \tfrac{1}{2}{E''_{qk}}^2\right]. \end{aligned} \tag{6.10}$$

### 6.2.2. Fourth- and third-order models

For the fourth-, third- (and second-)order model the transient reactances[7] $X'_{di}$ can be considered as part of the network (resulting in a different susceptance matrix, see Remark 5.8) implying that the energy in the transmission lines can be obtained by replacing the subtransient voltages by the transient voltages in Equation (6.10). For the third-order model $E'_{di} = 0$ for all $i \in \mathcal{V}$ so that the energy function associated with the transmission line between nodes $i$ and $k$ simplifies to

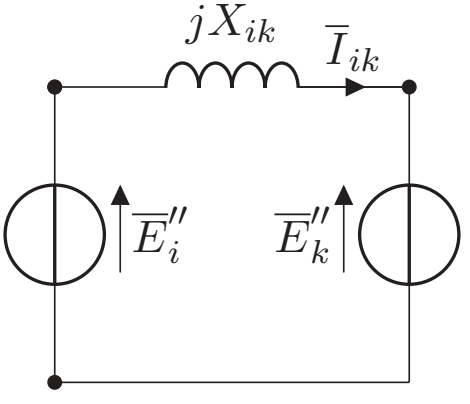


Figure 8. An inductive transmission line at steady state. The internal voltages $\bar{E}''_i, \bar{E}''_k$ are expressed in the corresponding local $dq0$-reference frame.

$$H_{ik} = -\frac{B_{ik}}{\omega_s}\left(\frac{1}{2}{E'_{qi}}^2 + \frac{1}{2}{E'_{qk}}^2 - E'_{qi}E'_{qk}\cos\delta_{ik}\right). \tag{6.11}$$

### 6.2.3. Second-order model

For the second-order model, it is convenient to represent transient voltages as $\bar{E}'_i = |\bar{E}'_i|e^{j\alpha_i}$ where $\alpha_i$ is the voltage angle of $\bar{E}'_i$ with respect to the rotor angle. Then, by defining the voltages angles $\theta_i = \delta_i + \alpha_i$ as in Section 5.3, the energy in the transmission line[8] Equation (6.10) takes the much simpler form

$$\begin{aligned} H_{ik} &= -\frac{B_{ik}}{2\omega_s}(\bar{E}'_i - \bar{E}'_k e^{-j\delta_{ik}})^*(\bar{E}'_i - \bar{E}'_k e^{-j\delta_{ik}}) \\ &= -\frac{B_{ik}}{2\omega_s}(|\bar{E}'_i|^2 - 2|\bar{E}'_i||\bar{E}'_k|\cos\theta_{ik} + |\bar{E}'_k|^2). \end{aligned} \tag{6.12}$$

## 6.3. Total energy

The total energy of the multi-machine system is equal to the sum of the previously mentioned energy functions

$$H = \sum_{i\in\mathcal{V}}(H_{di} + H_{qi} + H_{mi}) + \sum_{(i,k)\in\mathcal{E}} H_{ik}, \tag{6.13}$$

where the expressions for each individual energy function depends on the order of the model. The resulting energy function $H$ could serve as a candidate Lyaponuv function for the stability analysis of the multi-machine power network (with zero inputs).

**Remark 6.4** (Common factor $\omega_s^{-1}$ in energy functions) It is observed that each of the individual energy functions appearing in Equation (6.13) contains a factor $\omega_s^{-1}$. Therefore, a modified version of the energy function defined by $U = \omega_s H$ can also be used as a Lyapunov function for the multi-machine system. However, the function $U$ does not have the dimension of energy anymore, but has the dimension of power instead. In fact, in most of the literature these modified energy functions[9] (without the factor $\omega_s^{-1}$) are (part of) the collection of Lyapunov functions used to analyze the stability of the power network, see e.g. [4,11,13,15,18,32].

# 7. Port-Hamiltonian framework

By using the energy function established in the previous section, a convenient representation of the multi-machine models of Section 5 can be obtained. This is based on the theory of port-Hamiltonian systems, which yields a systematic framework for network modelling of multi-physics systems. In particular, we show in this section that the complex multi-machine systems Equations (5.6), (5.11) and (5.12) admit a simple port-Hamiltonian representation. Finally, some important passivity properties are proven for the resulting systems.

## 7.1. Sixth-order model

### 7.1.1. Energy in the transmission lines

Recall from Equation (6.10) that the energy stored in the inductive transmission line between node $i$ and $k$ is given by

$$\begin{aligned} H_{ik} &= -\tfrac{B_{ik}}{\omega_s}\big[\left(E''_{di}E''_{qk} - E''_{dk}E''_{qi}\right)\sin\delta_{ik} - \left(E''_{di}E''_{dk} + E''_{qi}E''_{qk}\right)\cos\delta_{ik} \\ &\quad + \tfrac{1}{2}{E''_{di}}^2 + \tfrac{1}{2}{E''_{dk}}^2 + \tfrac{1}{2}{E''_{qi}}^2 + \tfrac{1}{2}{E''_{qk}}^2\big]. \end{aligned} \tag{7.1}$$

Observe that the gradient of $H_{ik}$ takes the form

$$\begin{bmatrix} \frac{\partial H_{ik}}{\partial \delta_i} \\ \frac{\partial H_{ik}}{\partial E''_{qi}} \\ \frac{\partial H_{ik}}{\partial E''_{di}} \end{bmatrix} = \frac{B_{ik}}{\omega_s}\begin{bmatrix} (E''_{qi}E''_{dk} - E''_{di}E''_{qk})\cos\delta_{ik} - (E''_{di}E''_{dk} + E''_{qi}E''_{qk})\sin\delta_{ik} \\ -E''_{qi} + E''_{qk}\cos\delta_{ik} - E''_{dk}\sin\delta_{ik} \\ -E''_{di} + E''_{dk}\cos\delta_{ik} + E''_{qk}\sin\delta_{ik} \end{bmatrix}.$$

After defining the total energy stored in the transmission lines by $H_T = \sum_{(i,k)\in\mathcal{E}} H_{ik}$, we obtain likewise

$$\begin{aligned} \begin{bmatrix} \frac{\partial H_T}{\partial \delta_i} \\ \frac{\partial H_T}{\partial E''_{qi}} \\ \frac{\partial H_T}{\partial E''_{di}} \end{bmatrix} &= \frac{1}{\omega_s}\begin{bmatrix} \sum_{k\in\mathcal{N}_i} B_{ik}[(E''_{qi}E''_{dk} - E''_{di}E''_{qk})\cos\delta_{ik} - (E''_{di}E''_{dk} + E''_{qi}E''_{qk})\sin\delta_{ik}] \\ -B_{ii}E''_{qi} + \sum_{k\in\mathcal{N}_i} B_{ik}(E''_{qk}\cos\delta_{ik} + E''_{dk}\sin\delta_{ik}) \\ -B_{ii}E''_{di} + \sum_{k\in\mathcal{N}_i} B_{ik}(E''_{dk}\cos\delta_{ik} + E''_{qk}\sin\delta_{ik}) \end{bmatrix} \\ &= \frac{1}{\omega_s}\begin{bmatrix} P_{ei} \\ -I_{di} \\ I_{qi} \end{bmatrix} \end{aligned}$$

where we have used the fact that $B_{ii} = \sum_{k\in\mathcal{N}_i} B_{ik}$ and Equations (5.5) and (5.7).

### 7.1.2. Electrical energy synchronous machine

Further notice that the electrical energy stored in the $d$-axis in machine $i$ is given by

$$H_{di} = \frac{1}{2\omega_s}\begin{bmatrix} E'_{qi} & E''_{qi} \end{bmatrix}\begin{bmatrix} \frac{1}{X_{di}-X'_{di}} + \frac{1}{X'_{di}-X''_{di}} & -\frac{1}{X'_{di}-X''_{di}} \\ -\frac{1}{X'_{di}-X''_{di}} & \frac{1}{X'_{di}-X''_{di}} \end{bmatrix}\begin{bmatrix} E'_{qi} \\ E''_{qi} \end{bmatrix}$$

and satisfies

$$\begin{bmatrix} X_{di} - X'_{di} & X_{di} - X'_{di} \end{bmatrix}\begin{bmatrix} \frac{\partial H_{di}}{\partial E'_{qi}} \\ \frac{\partial H_{di}}{\partial E''_{qi}} \end{bmatrix} = \frac{1}{\omega_s}E'_{qi}$$

$$\begin{bmatrix} 0 & X'_{di} - X''_{di} \end{bmatrix}\begin{bmatrix} \frac{\partial H_{di}}{\partial E'_{qi}} \\ \frac{\partial H_{di}}{\partial E''_{qi}} \end{bmatrix} = \frac{1}{\omega_s}(E''_{qi} - E'_{qi}).$$

Observe that a similar result can be established for the energy function $H_{qi}$ by exchanging the $d$- and $q$-subscripts.

### 7.1.3. Mechanical energy

To obtain a port-Hamiltonian representation of the multi-machine models, it is convenient to rephrase and shift the energy function Equation (6.7) with respect to the synchronous frequency to obtain

$$\bar{H}_{mi} = \frac{1}{2} J_i \Delta\omega_i^2 = \frac{1}{2\omega_s} M_i \Delta\omega_i^2 = \frac{1}{2\omega_s} M_i^{-1} \mathrm{p}_i^2,$$

where $M_i = \omega_s J_i$ and we define the variable $\mathrm{p}_i = M_i \Delta\omega_i$.

**Remark 7.1** (Modified 'moment of inertia') Note that the quantity $\mathrm{p}_i$ does not represent the angular momentum of the synchronous machine but instead it is equal to $\mathrm{p}_i = \omega_s J \Delta\omega_i$ so it has a different physical dimension. In addition, it is shifted with respect to the synchronous frequency.

Using this definition of the Hamiltonian $\bar{H}_{mi}(\mathrm{p}_i)$, it follows that its gradient satisfies

$$\frac{\partial \bar{H}_{mi}}{\partial \mathrm{p}_i}(\mathrm{p}_i) = \frac{1}{\omega_s} M_i^{-1} \mathrm{p}_i = \frac{\Delta\omega_i}{\omega_s}.$$

### 7.1.4. Port-Hamiltonian representation

By the previous observations, the dynamics of a single synchronous machine in a multi-machine system Equation (5.6) can be written in the form

$$\begin{aligned}
\begin{bmatrix} \dot{\delta}_i \\ \dot{\mathrm{p}}_i \\ \dot{E}'_{qi} \\ \dot{E}'_{di} \\ \dot{E}''_{qi} \\ \dot{E}''_{di} \end{bmatrix} &= \omega_s \begin{bmatrix} 0 & 1 & 0 & 0 & 0 & 0 \\ -1 & 0 & 0 & 0 & 0 & 0 \\ 0 & 0 & -\frac{\hat{X}_{di}}{T'_{doi}} & 0 & -\frac{\hat{X}_{qi}}{T'_{qoi}} & 0 \\ 0 & 0 & 0 & -\frac{\hat{X}_{di}}{T'_{doi}} & 0 & -\frac{\hat{X}_{qi}}{T'_{qoi}} \\ 0 & 0 & 0 & 0 & -\frac{\hat{X}'_{di}}{T''_{doi}} & 0 \\ 0 & 0 & 0 & 0 & 0 & -\frac{\hat{X}'_{qi}}{T''_{qoi}} \end{bmatrix} \nabla_i H + \begin{bmatrix} 0 & 0 \\ 1 & 0 \\ 0 & \frac{1}{T'_{doi}} \end{bmatrix} 000000 \underbrace{\begin{bmatrix} P_{mi} \\ E_{fi} \end{bmatrix}}_{u_i} \\
y_i &= \begin{bmatrix} 0 & 1 & 0 & 0 & 0 & 0 \\ 0 & 0 & \frac{1}{T'_{doi}} & 0 & 0 & 0 \end{bmatrix} \nabla_i H
\end{aligned} \tag{7.2}$$

where

$$H = \sum_{i \in \mathcal{V}} (\bar{H}_{mi} + H_{di} + H_{qi}) + \sum_{(i,k) \in \mathcal{E}} H_{ik}$$

and $\hat{X}_{di} := X_{di} - X'_{di}, \hat{X}'_{di} := X'_{di} - X''_{di}, \hat{X}_{qi} := X_{qi} - X'_{qi}, \hat{X}'_{qi} := X'_{qi} - X''_{qi}$ and $\nabla_i H$ denotes the gradient of $H$ with respect to the variables $\mathrm{col}(\delta_i, \mathrm{p}_i, E'_{qi}, E'_{di}, E''_{qi}, E''_{di})$. Note that the mechanical energy $\bar{H}_{mi}$ is *shifted* around the synchronous frequency.

By aggregating the states of the synchronous machines, i.e. $\delta = \mathrm{col}(\delta_1, \ldots, \delta_n)$ etc., the multi-machine system is described by

$$\begin{bmatrix} \dot{\delta} \\ \dot{\mathrm{p}} \\ \dot{E}'_q \\ \dot{E}'_d \\ \dot{E}''_q \\ \dot{E}''_d \end{bmatrix} = \omega_s \underbrace{\begin{bmatrix} 0 & I & 0 & 0 & 0 & 0 \\ -I & 0 & 0 & 0 & 0 & 0 \\ 0 & 0 & -(T'_{do})^{-1}\hat{X}_d & 0 & -(T'_{do})^{-1}\hat{X}_d & 0 \\ 0 & 0 & 0 & -(T'_{qo})^{-1}\hat{X}_q & 0 & -(T'_{qo})^{-1}\hat{X}_q \\ 0 & 0 & 0 & 0 & -(T''_{do})^{-1}\hat{X}'_d & 0 \\ 0 & 0 & 0 & 0 & 0 & -(T''_{qo})^{-1}\hat{X}'_q \end{bmatrix}}_{J-R} \nabla H + g \underbrace{\begin{bmatrix} P_m \\ E_f \end{bmatrix}}_{u}, \quad y = g^T \nabla H, \quad g = \begin{bmatrix} 0 & I & 0 & 0 & 0 & 0 \\ 0 & 0 & (T'_{do})^{-1} & 0 & 0 & 0 \end{bmatrix}^T, \tag{7.3}$$

where $\hat{X}_d = \mathrm{diag}(\hat{X}_{d1}, \ldots, \hat{X}_{dn})$, $T'_{do} = \mathrm{diag}(T'_{do1}, \ldots, T'_{don})$ and likewise definitions are used for the quantities $\hat{X}'_d, \hat{X}_q, \hat{X}'_q, T'_{qo}, T''_{do}, T''_{qo}$. The matrix $J - R$ depicted in Equation (7.3) consists of a skew-symmetric matrix $J = -J^T$ and a symmetric matrix $R = R^T$ often called the *dissipation matrix* [1].

**Remark 7.2** (Port-Hamiltonian structures of 6th- and 9th-order models) By comparing the port-Hamiltonian structures (i.e. the $J$ and $R$ matrices) of the 6th- and 9th-order models we see several fundamental changes. First, compared to the first-principle model, in the 6th-order model there is no interconnection structure present between electrical and mechanical part of the system (and therefore we expect lesser oscillatory behavior between the two subsystems, see also Remark 4.2). Instead, for a multi-machine model, in the 6th-order model this coupling comes through the Hamiltonian, in particular from the part corresponding to the transmission line energy.

Another fundamental change compared to the full-order model is that self-interconnection and self-dissipation structure of the electrical part of the system is different. Specifically, for the first-principle model, there is only a resistive structure present while in the sixth-order model also a nonzero interconnection structure is present. We argue that the reason for this difference comes from the somewhat contradiction Assumptions 4.6, 4.7 in Section 4.2. In addition, dissipation structure of the sixth-order model is not diagonal anymore compared to the full-order model due to the fact that state transformation is not 'diagonal', see the definitions of $E''_q, E''_d$ in Section 4.2.2 (observe from Equation (4.9) for example that $E_{q''}$ not only depends on $\Psi_D$ but also on $\Psi_f$). Furthermore, for the sixth-order model, it is not immediate that this dissipation matrix is positive (semi)-definite. This is needed to verify that the system Equation (7.3) is indeed a port-Hamiltonian representation of the sixth-order multi-machine network Equation (5.6).

**Proposition 7.3** (System:6multiphall is port-Hamiltonian with $R \geq 0$). Equation (7.3) *defines a port-Hamiltonian representation of the 6th-order multi-machine network Equation (5.6). In particular, the matrix R is positive semi-definite.*

***Proof.*** The dissipation matrix of the system Equation (7.3) is equal to the symmetric part of the matrix in Equation (7.3) and amounts to

$$R = \omega_s \begin{bmatrix} 0 & 0 & 0 & 0 & 0 & 0 \\ 0 & 0 & 0 & 0 & 0 & 0 \\ 0 & 0 & (T'_{do})^{-1}\hat{X}_d & 0 & \frac{1}{2}(T'_{do})^{-1}\hat{X}_d & 0 \\ 0 & 0 & 0 & (T'_{qo})^{-1}\hat{X}_q & 0 & \frac{1}{2}(T'_{qo})^{-1}\hat{X}_q \\ 0 & 0 & \frac{1}{2}(T'_{do})^{-1}\hat{X}_d & 0 & (T''_{do})^{-1}\hat{X}'_d & 0 \\ 0 & 0 & 0 & \frac{1}{2}(T'_{qo})^{-1}\hat{X}_q & 0 & (T''_{qo})^{-1}\hat{X}'_q \end{bmatrix}.$$

By invoking the Schur complement, $R = R^T \geq 0$ if and only if

$$\begin{bmatrix} 2\frac{X_{di}-X'_{di}}{T'_{doi}} & \frac{X_{di}-X'_{di}}{T'_{doi}} \\ \frac{X_{di}-X'_{di}}{T'_{doi}} & 2\frac{X'_{di}-X''_{di}}{T''_{doi}} \end{bmatrix} \geq 0 \quad \text{and} \quad \begin{bmatrix} 2\frac{X_{qi}-X'_{qi}}{T'_{qoi}} & \frac{X_{qi}-X'_{qi}}{T'_{qoi}} \\ \frac{X_{qi}-X'_{qi}}{T'_{qoi}} & 2\frac{X'_{qi}-X''_{qi}}{T''_{qoi}} \end{bmatrix} \geq 0, \quad \forall i \in \mathcal{V},$$

which holds if and only if

$$4(X'_{di} - X''_{di})T'_{doi} - (X_{di} - X'_{di})T''_{doi} \geq 0, \tag{7.4a}$$

$$4(X'_{qi} - X''_{qi})T'_{qoi} - (X_{qi} - X'_{qi})T''_{qoi} \geq 0, \tag{7.4b}$$

holds for all $i \in \mathcal{V}$. By substituting the quantities from Equation (4.2) and simplying the equations using computer algebra program Mathematica 11, we obtain

$$\begin{aligned} &4(X'_{di} - X''_{di})T'_{doi} - (X_{di} - X'_{di})T''_{doi} \\ &= \kappa^2\omega_s \cdot \frac{4L_f^2(L_fM_D - L_{fD}M_f)^2R_D + (L_DL_f - L_{fD}^2)^2M_f^2R_f}{L_f^2(L_DL_f - L_{fD}^2)R_DR_f}\Big|_i > 0 \end{aligned} \tag{7.5a}$$

$$\begin{aligned} &4(X'_{qi} - X''_{qi})T'_{qoi} - (X_{qi} - X'_{qi})T''_{qoi} \\ &= \kappa^2\omega_s \cdot \frac{4L_g^2(L_gM_Q - L_{gQ}M_g)^2R_Q + (L_QL_g - L_{gQ}^2)^2M_g^2R_g}{L_g^2(L_QL_g - L_{gQ}^2)R_QR_g}\Big|_i > 0 \end{aligned} \tag{7.5b}$$

where by $|_i$ we mean the constants (e.g. $L_f, L_g$) associated to machine $i \in \mathcal{V}$. We claim that the inequality holds in Equation (7.5). This follows from the fact for a realistic synchronous machine we have that $R_D, R_Q, R_f, R_g, L_f, L_g, L_D, L_Q > 0$ and, since $X_q - X'_q > 0, X_d - X'_d > 0$ (see Remark 4.4), we have that $M_f \neq 0, M_g \neq 0$. In addition, $L_DL_f - L_{fD}^2 > 0, L_QL_g - L_{fQ}^2 > 0$ as the inductance matrices $\mathcal{L}_d, \mathcal{L}_q$ defined in Equations (3.2) and (3.3) are positive definite. Hence, Equation (7.4) holds in the strict sense and consequently $R$ is positive semi-definite and therefore Equation (7.3) defines a port-Hamiltonian system.

**Remark 7.4** (Hamiltonian representations of 5th- and 4th-order models) We can show that similar port-Hamiltonian structures appear for the 5th- and 4th-order multi-machine networks using the corresponding (shifted) energy functions derived in

Section 6 and Section 7.1.3 as the Hamiltonian. Specifically, we can verify that the interconnection and damping matrices for the 5th-order model are given by

$$J - R = \omega_s \begin{bmatrix} 0 & I & 0 & 0 & 0 \\ -I & 0 & 0 & 0 & 0 \\ 0 & 0 & -(T'_{do})^{-1}\hat{X}_d & -(T'do)^{-1}\hat{X}_d & 0 \\ 0 & 0 & 0 & -(T''_{do})^{-1}\hat{X}'_d & 0 \\ 0 & 0 & 0 & 0 & -(T''_{qo})^{-1}\hat{X}'_q \end{bmatrix},$$
$$g = \begin{bmatrix} 0 & 0 \\ I & 0 \\ 0 & (T'_{do})^{-1} \\ 0 & 0 \\ 0 & 0 \end{bmatrix} \tag{7.6}$$

and for the fourth-order model these take the form

$$J - R = \omega_s \begin{bmatrix} 0 & I & 0 & 0 \\ -I & -D & 0 & 0 \\ 0 & 0 & -(T'_{do})^{-1}\hat{X}_d & 0 \\ 0 & 0 & 0 & -(T'_{qo})^{-1}\hat{X}_q \end{bmatrix}, \quad g = \begin{bmatrix} 0 & 0 \\ I & 0 \\ 0 & (T'_{do})^{-1} \\ 0 & 0 \end{bmatrix}. \tag{7.9}$$

In particular, we observe that for fifth-order model also a nontrivial interconnection and damping structure is present. Similarly, in Proposition 7.3 we can verify the positive semi-definiteness of the dissipation matrix $R$ but now only using Equation (7.5a). For the fourth-order model, we observe again a diagonal dissipation matrix as also apparent in the full-order model (3.5).

For the third-order model we now give a more detailed derivation of its port-Hamiltonian representation.

## 7.2. Third-order model

Recall from (6.11) that the energy stored in the inductive transmission line between node $i$ and $k$ is given by

$$H_{ik} \quad = -\frac{B_{ik}}{\omega_s}\left(\tfrac{1}{2}{E'_{qi}}^2 + \tfrac{1}{2}{E'_{qk}}^2 - E'_{qi}E'_{qk}\cos\delta_{ik}\right). \tag{7.8}$$

Observe that the gradient of $H_{ik}$ is given by

$$\begin{bmatrix} \frac{\partial H_{ik}}{\partial \delta_i} \\ \frac{\partial H_{ik}}{\partial E'_{qi}} \end{bmatrix} = \frac{B_{ik}}{\omega_s}\begin{bmatrix} -E'_{qi}E'_{qk}\sin\delta_{ik} \\ -E'_{qi} + E'_{qk}\cos\delta_{ik} \end{bmatrix}.$$

Define now the total energy stored in the transmission lines by $H_T = \sum_{(i,k)\in\mathcal{E}} H_{ik}$. Then we obtain likewise

$$\begin{bmatrix} \frac{\partial H_T}{\partial \delta_i} \\ \frac{\partial H_T}{\partial E'_{qi}} \end{bmatrix} = \frac{1}{\omega_s} \begin{bmatrix} \sum_{k\in\mathcal{N}_i} B_{ik} - E'_{qi}E'_{qk}\sin\delta_{ik} \\ -B_{ii}E'_{qi} + \sum_{k\in\mathcal{N}_i} B_{ik}E'_{qk}\cos\delta_{ik} \end{bmatrix} = \frac{1}{\omega_s}\begin{bmatrix} P_{ei} \\ -I_{di} \end{bmatrix}.$$

Further notice that the electrical energy stored in machine $i$ is given by

$$H_{dqi} = \frac{1}{2\omega_s}\frac{{E'_{qi}}^2}{X_{di} - X'_{di}}$$

and satisfies

$$(X_{di} - X'_{di})\frac{\partial H_{dqi}}{\partial E'_{qi}} = \frac{1}{\omega_s}E'_{qi}.$$

By the previous observations and aggregating the states, the dynamics of the third-order multi-machine system Equation (5.11) can now be written in port-Hamiltonian form as

$$\begin{aligned} \begin{bmatrix} \dot{\delta} \\ \dot{\mathrm{p}} \\ \dot{E}'_q \end{bmatrix} &= \omega_s \begin{bmatrix} 0 & I & 0 \\ -I & -D & 0 \\ 0 & 0 & -(T'_{do})^{-1}(X_d - X'_d) \end{bmatrix} \nabla H + g \underbrace{\begin{bmatrix} P_m \\ E_f \end{bmatrix}}_{u}, \\ y &= g^T \nabla H, \quad g^T = \begin{bmatrix} 0 & I & 0 \\ 0 & 0 & (T'_{do})^{-1} \end{bmatrix}, \quad H = \sum_{i\in\mathcal{V}}(\bar{H}_{mi} + H_{dqi}) + \sum_{(i,k)\in\mathcal{E}} H_{ik} \end{aligned} \tag{7.9}$$

where $X_d = \mathrm{diag}(X_{d1}, \ldots, X_{dn}), X'_d = \mathrm{diag}(X'_{d1}, \ldots, X'_{dn})$, and in addition $T'_{do} = \mathrm{diag}(T'_{do1}, \ldots, T'_{don})$.

### 7.3. Swing equations

Recall from Equation (6.12) that the energy stored in the inductive transmission line between node $i$ and $k$ is given by

$$H_{ik} \quad = \quad = -\tfrac{B_{ik}}{2\omega_s}\left(\left|\bar{E}'_i\right|^2 - 2\left|\bar{E}'_i\right|\left|\bar{E}'_k\right|\cos\theta_{ik} + \left|\bar{E}'_k\right|^2\right). \tag{7.10}$$

Define now the total energy stored in the transmission lines by $H_T = \sum_{(i,k)\in\mathcal{E}} H_{ik}$ and observe that the gradient of $H_T$ with respect to the transformed angle $\theta$ is given by

$$\frac{\partial H_T}{\partial \theta_i} = -\sum_{j\in\mathcal{N}_i}\frac{B_{ik}}{\omega_s}\left|\bar{E}'_i\right|\left|\bar{E}'_k\right|\sin\theta_{ik}.$$

For the second-order model the electrical energy stored in the generator circuits is constant and can therefore be omitted from the Hamiltonian without loss of generality. By the previous observations and aggregating the states, the dynamics of the second-order multi-machine system Equation (5.12) can be written in port-Hamiltonian form as

$$\begin{aligned} \begin{bmatrix} \dot{\delta} \\ \dot{\mathrm{p}} \end{bmatrix} &= \omega_s \begin{bmatrix} 0 & I \\ -I & -D \end{bmatrix} \nabla H + \begin{bmatrix} 0 \\ I \end{bmatrix} \underbrace{P_m}_{u} \\ y &= \begin{bmatrix} 0 & I \end{bmatrix} \nabla H = \tfrac{\Delta\omega}{\omega_s}, \qquad H = \sum_{i\in\mathcal{V}} \bar{H}_{mi} + \sum_{(i,k)\in\mathcal{E}} H_{ik}. \end{aligned} \tag{7.11}$$

### 7.4. Shifted passivity

In this section we establish the shifted passivity properties of the reduced-order multi-machine models.

**Definition 7.5** (Shifted passivity) Let $(\bar{x}, \bar{u}, \bar{y})$ be such that $f(\bar{x}, \bar{u}) = 0, \bar{y} = h(\bar{x}, \bar{u})$. Then $\dot{x} = f(x, u), y = h(x, u)$ where $x \in \mathcal{D} \subset \mathbb{R}^n$ is shifted passive with respect to the shifted input-output pair $(u - \bar{u}, y - \bar{y})$ if there exists a differentiable storage function $V : \mathcal{D} \to \mathbb{R}_{\geq 0}$ satisfying the differential dissipation inequality

$$\frac{d}{dt} V(x(t)) = (\nabla V(x(t)))^T f(x(t), u(t)) \leq (u(t) - \bar{u})^T (y(t) - \bar{y})$$

for all solutions $x(.)$ corresponding to input functions $u(.)$.

**Proposition 7.6** (Shifted passivity of reduced-order models) *The 6,5,4,3, and 2nd-order multi-machine models are shifted passive using the local storage function* $\bar{H}(x) := H(x) - (x - \bar{x})^T \nabla H(\bar{x}) - H(\bar{x})$, *provided that a steady state* $(\bar{x}, \bar{u}, \bar{y})$ *exists with* $\nabla^2 H(\bar{x}) \geq 0$ *where* $H$ *is defined as in Section 6.*

***Proof.*** We first observe that the multi-machine systems Equations (7.3), (7.9) and (7.11) (but also the 5th- and 4th-order models, see Remark 7.4) can be written in the port-Hamiltonian form

$$\begin{aligned} \dot{x} &= (J - R)\nabla H(x) + gu \\ y &= g^T \nabla H(x) \end{aligned} \tag{7.12}$$

with constant matrices $J = -J^T, R = R^T \geq 0$, see also Proposition 7.3. Let $(\bar{x}, \bar{u}, \bar{y})$ correspond to a steady state of Equation (7.12), i.e.

$$0 = (J - R)\nabla H(\bar{x}) + g\bar{u}$$

$$\bar{y} = g^T \nabla H(\bar{x})$$

and suppose that $\nabla^2 H(\bar{x}) \geq 0$. Define the *shifted Hamiltonian* (see e.g. [1]) as $\bar{H}(x) := H(x) - (x - \bar{x})^T \nabla H(\bar{x}) - H(\bar{x})$ as in the proposition. Then the system Equation (7.12) can be rewritten as

$$\dot{x} = (J - R)\nabla \bar{H}(x) + g(u - \bar{u})$$

$$y - \bar{y} = g^T \nabla \bar{H}(x).$$

The shifted passivity follows by taking the time-derivative of the shifted Hamiltonian $\bar{H}$ which yields

$$\dot{\bar{H}} = -(\nabla \bar{H}(x))^T R \nabla \bar{H}(x) + (u - \bar{u})^T (y - \bar{y}) \leq (u - \bar{u})^T (y - \bar{y}).$$

Since in addition $\bar{H}(\bar{x}) = 0, \nabla H(\bar{x}) = 0$ and $\nabla^2 \bar{H}(\bar{x}) = \nabla^2 H(\bar{x}) \geq 0$, it follows that $\bar{H}$ is a suitable local storage function.

**Remark 7.7** (Hessian condition) To use Proposition 7.6 one must verify that the Hessian of the Hamiltonian evaluated at the (desired) equilibrium is positive semi-definite. For the second- and third-order multi-machine models a sufficient condition is established for guaranteeing that the Hessian is positive definite, see [19,33]. It can be verified that these conditions hold for a typical operation point of the power network, i.e. for which the voltage (angle) differences are small. However, further effort is required to establish a similar condition for the higher-order multi-machine models, which preferably can be checked in a distributed fashion.

The shifted passivity property mentioned in Proposition 7.6 that the previously derived multi-machine models (7.3), (7.9), (7.11) (and the 5th-, and 4th-order models) admit proves to be very useful when interconnection with (passive and optimal) controllers, see in particular our previous work [5,22] for an analysis of the third- and sixth-order models respectively.

## 8. Conclusions and future research

In this article, a unifying energy-based approach to the modelling of multi-machine power networks is provided. Starting from the first-principle model of the synchronous generator, reduced order models are obtained and the underlying assumptions are explained. After determining the energy functions of the reduced-order models, a port-Hamiltonian representation of the multi-machine systems is established. In particular, it is shown that advanced multi-machine models that are much more advanced can be analyzed using the port-Hamiltonian framework. Moreover, the resulting port-Hamiltonian system is proven to be shifted passive with respect to its steady states. The latter property has turned out to be crucial in many contexts, in particular for the stability analysis of the (optimal) equilibria of the closed-loop system [5,18,19].

### 8.1. Future research

The results established in this article can be extended in many possible ways. We elaborate on the main research directions in the following.

#### 8.1.1. Control

One natural extension of the work established in the present article is to consider (distributed) control of multi-machine networks. For frequency control, this can for example be done following the lines of [18,22,34]. Since in the present article we established a systematic way for obtaining the energy functions and proved (shifted) passivity of the system, we conjecture that the same kind of controllers established in these references can be applied to (purely inductive) multi-machine models where each synchronous machine is described by a 2,3,4,5 or 6th-order model. In particular, the 6th-order multi-machine case was already been in our previous work [22]. Alternatively, one can continue along the lines of [4,5,11,35] and consider controllers based on the primal-dual gradient method. In addition, further effort is required to investigate the possibilities of (optimal) voltage control using passive controllers. One possibility is to extend the work of [19,20] to high-dimensional multi-machine models.

### 8.1.2. Nonzero transfer conductances

Another extension to this work is to include transmission line resistances in the network. However, in [10,36] and references therein it is observed that in the case of nonzero transfer conductances, a Lyapunov based stability analysis can be cumbersome and involves adding nontrivial cross terms in the Lyapunov function. Even then, the stability analysis relies on a 'sufficiently small transfer conductances' assumption [10,36]. On the other hand, one approach that could be adopted in future research is to assume the resistive transmission lines are uniform such that the $R/X$ ratios are identical for all transmission lines. This simplifies the analysis and possibly the present work could be extended to this case (and keeping the port-Hamiltonian structure intact), for example by following the lines of [19] and references therein.

### 8.1.3. More accurate power network models

In the present article, we considered the case that each node in the network represents a synchronous machine. A natural extension is to generalize the established results to the case where some of the nodes represent inverters or (frequency-dependent) loads instead. In addition, while advanced models of the synchronous generator are considered in this article, there are many possible extensions to these models. For example, models for the turbine and speed governor as considered in e.g. [30,35,37] could also be taken into account. Finally, the model can be expanded such that the excitation system and the automatic voltage regulator (AVR) are included as well [7].

## Notes

1. Text for Footnote 1This is in contrast to [8,26] where the convention $\bar{V} = V_d + jV_q$ is used.
2. Text for Footnote 1See in particular [7], Chapter 11] for a\$146#detailed derivation of the model (1).
3. Text for Footnote 1For example, in Europe the synchronous frequency is 50Hz and in the United States it is 60.
4. Text for Footnote 1Note that the angle $\theta_i$ represents the *voltage angle* of generator $i$ with respect to the synchronous rotating reference frame.
5. Text for Footnote 1Note that for the third-order model $\alpha_i = 0$ implying that in this case $\theta_i$ is equal to the rotor angle $\delta_i$ with respect to the synchronous rotating reference frame.
6. Text for Footnote 1For notational convenience the subscript $i$ is omitted in this section.
7. Text for Footnote 1Provided that the transient saliency is neglected, i.\$132#e. $X'_{di} = X'_{qi}$ for all $i \in \mathcal{V}$.
8. Text for Footnote 1Where the subtransient voltages are replaced by the transient voltages.
9. Text for Footnote 1Which are sometimes incorrectly called *energy functions* as well.

## Disclosure statement

No potential conflict of interest was reported by the authors.

## Funding

This work is supported by the Netherlands Organisation for Scientific Research (NWO) programme Uncertainty Reduction in Smart Energy Systems (URSES) under the auspices of the project Energy-based analysis and control of the grid: dealing with uncertainty and markets (ENBARK);Stichting voor de Technische Wetenschappen [URSES, ENBARK].

## ORCID

T. W. Stegink http://orcid.org/0000-0002-0275-811X

## References

[1] A.J. van der Schaft and D. Jeltsema, *Port-Hamiltonian systems theory: An introductory overview*, Found. Trends Syst. Control 1 (2014), pp. 173–378. doi:10.1561/2600000002.
[2] S. Fiaz, D. Zonetti, R. Ortega, J.M.A. Scherpen, and A.J. van der Schaft, *A port-Hamiltonian approach to power network modeling and analysis, European*, J. Control. 19(2013), pp. 477–485
[3] T.W. Stegink, C. De Persis, and A.J. van der Schaft, *A port-Hamiltonian approach to optimal frequency regulation in power grids*, IEEE Conference on Decision and Control, Osaka, Japan, 2015, pp. 3224–3229.
[4] T.W. Stegink, C. De Persis, and A.J. van der Schaft, *Port-Hamiltonian formulation of the gradient method applied to smart grids*, IFAC-PapersOnLine 48 (2015), pp. 13–18. doi:10.1016/j.ifacol.2015.10.207.
[5] T.W. Stegink, C. De Persis, and A.J. van der Schaft, *A unifying energy-based approach to stability of power grids with market dynamics*, IEEE Trans Automat Contr 62 (2017), pp. 2612–2622. doi:10.1109/TAC.2016.2613901.
[6] P.M. Anderson and A.A. Fouad, *Power System Control and Stability*, 1st ed., The Iowa State Univsersity Press, Iowa City, Iowa, USA, 1977.
[7] J. Machowski, J.W. Bialek, and J.R. Bumby, *Power System Dynamics: Stability and Control*, 2nd ed., John Wiley & Sons, Ltd., Hoboken, 2008.
[8] P. Kundur, *Power System Stability and Control*, Mc-Graw-Hill Engineering, New York, 1993.
[9] S.Y. Caliskan and P. Tabuada, *Compositional transient stability analysis of multimachine power networks*, IEEE Trans. Control Network Syst. 1 (2014), pp. 4–14. doi:10.1109/TCNS.2014.2304868.
[10] R. Ortega, M. Galaz, A. Astolfi, Y. Sun, and T. Shen, *Transient stabilization of multimachine power systems with nontrivial transfer conductances*, IEEE Trans Automat Contr 50 (2005), pp. 60–75. doi:10.1109/TAC.2004.840477.
[11] N. Li, L. Chen, C. Zhao, and S.H. Low, Connecting automatic generation control and economic dispatch from an optimization view, American Control Conference, IEEE, Portland, OR, USA, 2014, pp. 735–740.
[12] Y. Seungil and C. Lijun, *Reverse and forward engineering of frequency control in power networks*, Proceeding of IEEE Conference on Decision and Control, Los Angeles, CA, USA, 2014.
[13] X. Zhang and A. Papachristodoulou, *A real-time control framework for smart power networks: Design methodology and stability*, Autom. 58 (2015), pp. 43–50. doi:10.1016/j.automatica.2015.05.003.
[14] C. Zhao, E. Mallada, and S.H. Low, *Distributed generator and load-side secondary frequency control in power networks*, 49th Annual Conference on Information Sciences and Systems (CISS), IEEE, Baltimore, Maryland, 2015, pp. 1–6.

[15] M. Pai, Energy Function Analysis for Power System Stability, Springer Science & Business Media, Berlin, 1989.
[16] A. Fouad and S. Stanton, *Transient Stability of a Multi-Machine Power System Part I: Investigation of System Trajectories, IEEE Transactions on Power Apparatus and Systems*, IEEE, 1981, pp. 3408–3416.
[17] A. Michel, A. Fouad, and V. Vittal, *Power system transient stability using individual machine energy functions*, IEEE EEE Trans. Circuits Syst. 30 (1983), pp. 266–276. doi:10.1109/TCS.1983.1085360.
[18] S. Trip, M. Bürger, and C. De Persis, *An internal model approach to (optimal) frequency regulation in power grids with time-varying voltages*, Autom. 64 (2016), pp. 240–253. doi:10.1016/j.automatica.2015.11.021.
[19] C. De Persis and N. Monshizadeh, *Bregman storage functions for microgrid control*, IEEE Trans Automat Contr 63 (2018), pp. 53–68. doi:10.1109/TAC.2017.2709246.
[20] C. De Persis, N. Monshizadeh, J. Schiffer, and F. Dörfler, A Lyapunov approach to control of microgrids with a network-preserved differential-algebraic model, IEEE Conference on Decision and Control, Las Vegas, NV, USA, 2016, pp. 2595–2600.
[21] S.Y. Caliskan and P. Tabuada, *Uses and abuses of the swing equation model*, IEEE Conference on Decision and Control, Osaka, Japan, 2015, pp. 6662–6667.
[22] T.W. Stegink, C. De Persis, and A.J. van der Schaft, *Optimal power dispatch in networks of high-dimensional models of synchronous machines*, IEEE Conference on Decision and Control, IEEE, Las Vegas, NV, USA, 2016, pp. 4110–4115.
[23] J. Schiffer, D. Zonetti, R. Ortega, A.M. Stanković, T. Sezi, and J. Raisch, *A survey on modeling of microgrids-From fundamental physics to phasors and voltage sources*, Autom. 74 (2016), pp. 135–150. doi:10.1016/j.automatica.2016.07.036.
[24] A.J. van der Schaft and T.W. Stegink, *Perspectives in modeling for control of power networks*, Annu. Rev. Control 41 (2016), pp. 119–132. doi:10.1016/j.arcontrol.2016.04.017.
[25] B. Maschke, R. Ortega, and A.J. Van Der Schaft, *Energy-based Lyapunov functions for forced Hamiltonian systems with dissipation*, IEEE Trans. Automat. Contr. 45 (2000), pp. 1498–1502. doi:10.1109/9.871758.
[26] P.W. Sauer and M.A. Pai, *Power System Dynamics and Stability*, Prentice-Hall, Upper Saddle River, New Jersey, 1998.
[27] S. Ahmed-Zaid, P.W. Sauer, M.A. Pai, and M.K. Sarioglu, *Reduced order modeling of synchronous machines using singular perturbation*, IEEE EEE Trans. Circuits Syst. 29 (1982), pp. 782–786. doi:10.1109/TCS.1982.1085101.
[28] P.V. Kokotovic, J.J. Allemong, J.R. Winkelman, and J.H. Chow, *Singular perturbation and iterative separation of time scales*, Autom. 16 (1980), pp. 23–33. doi:10.1016/0005-1098(80)90083-7.
[29] R.H. Park, *Two-reaction theory of synchronous machines generalized method of analysis-part I*, IEEE Trans. Am. Inst. Electr. Eng. 48 (1929), pp. 716–727. doi:10.1109/T-AIEE.1929.5055275.
[30] F.L. Alvarado, J. Meng, C.L. DeMarco, and W.S. Mota, *Stability analysis of interconnected power systems coupled with market dynamics*, IEEE Trans. Power Syst. 16 (2001), pp. 695–701. doi:10.1109/59.962415.
[31] A.R. Bergen and D.J. Hill, *Structure Preserving Model for Power System Stability Analysis, IEEE Transaction on Power Apparatus and Systems PAS-100*, IEEE, 1981, pp. 25–35.
[32] X. Zhang and A. Papachristodoulou, A real-time control framework for smart power networks with star topology, American Control Conference, IEEE, Washington DC, 2013, pp. 5062–5067.
[33] M. Bürger, C. De Persis, and S. Trip, An internal model approach to (optimal) frequency regulation in power grids, Proceedings of the MTNS, Groningen, 2014, pp. 577–583.
[34] J.W. Simpson-Porco, F. Dörfler, and F. Bullo, *Synchronization and power sharing for droop-controlled inverters in islanded microgrids*, Autom. 49 (2013), pp. 2603–2611. doi:10.1016/j.automatica.2013.05.018.

[35] X. Zhang, N. Li, and A. Papachristodoulou, *Achieving Real-Time Economic Dispatch in Power Networks via a Saddle Point Design Approach, in Power & Energy Society General Meeting*, IEEE, Denver, CO, USA, 2015, pp. 1–5.
[36] N.G. Bretas and L.F. Alberto, *Lyapunov function for power systems with transfer conductances: Extension of the invariance principle*, IEEE Trans. Power Syst. 18 (2003), pp. 769–777. doi:10.1109/TPWRS.2003.811207.
[37] S. Trip and C. De Persis, Distributed Optimal Load Frequency Control with Non-Passive Dynamics, IEEE Transactions on Control of Network Systems, IEEE, 2017.